

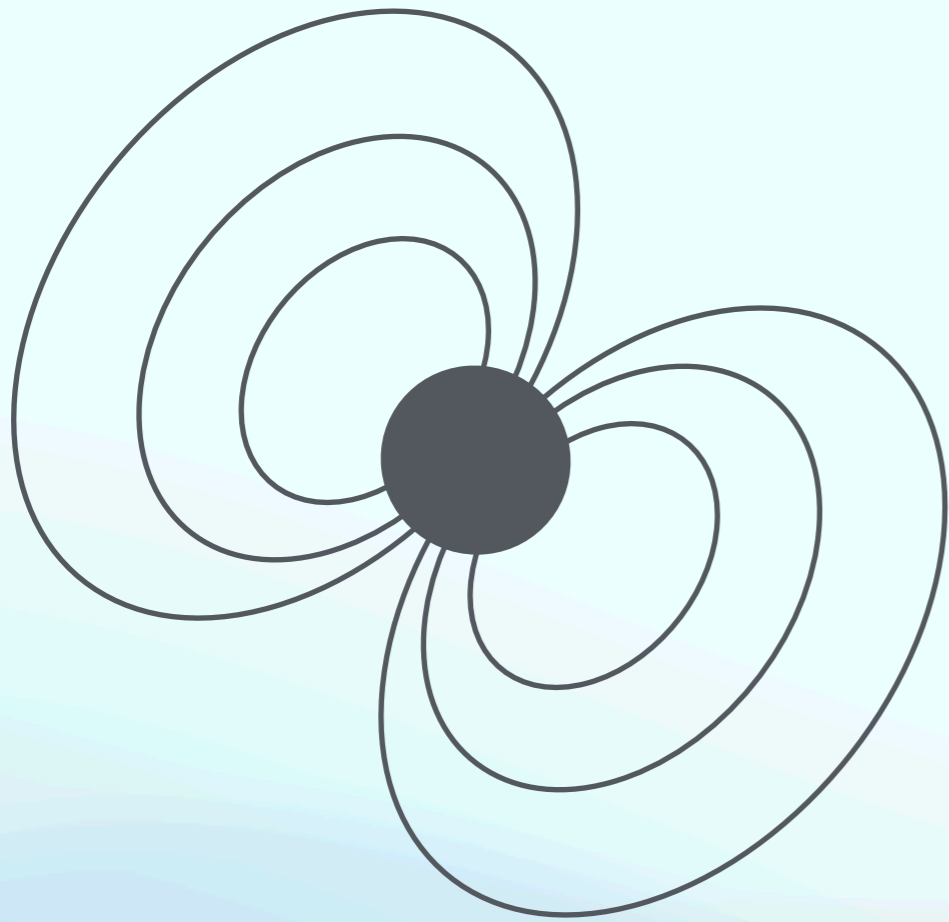
Neutron star populations in the Galaxy and their evolutionary interconnection

Stefano Ascenzi (Gran Sasso Science Institute)

Outline

- Introduction
- The neutron star zoo
- Magneto-thermal evolution
- Summary and conclusion

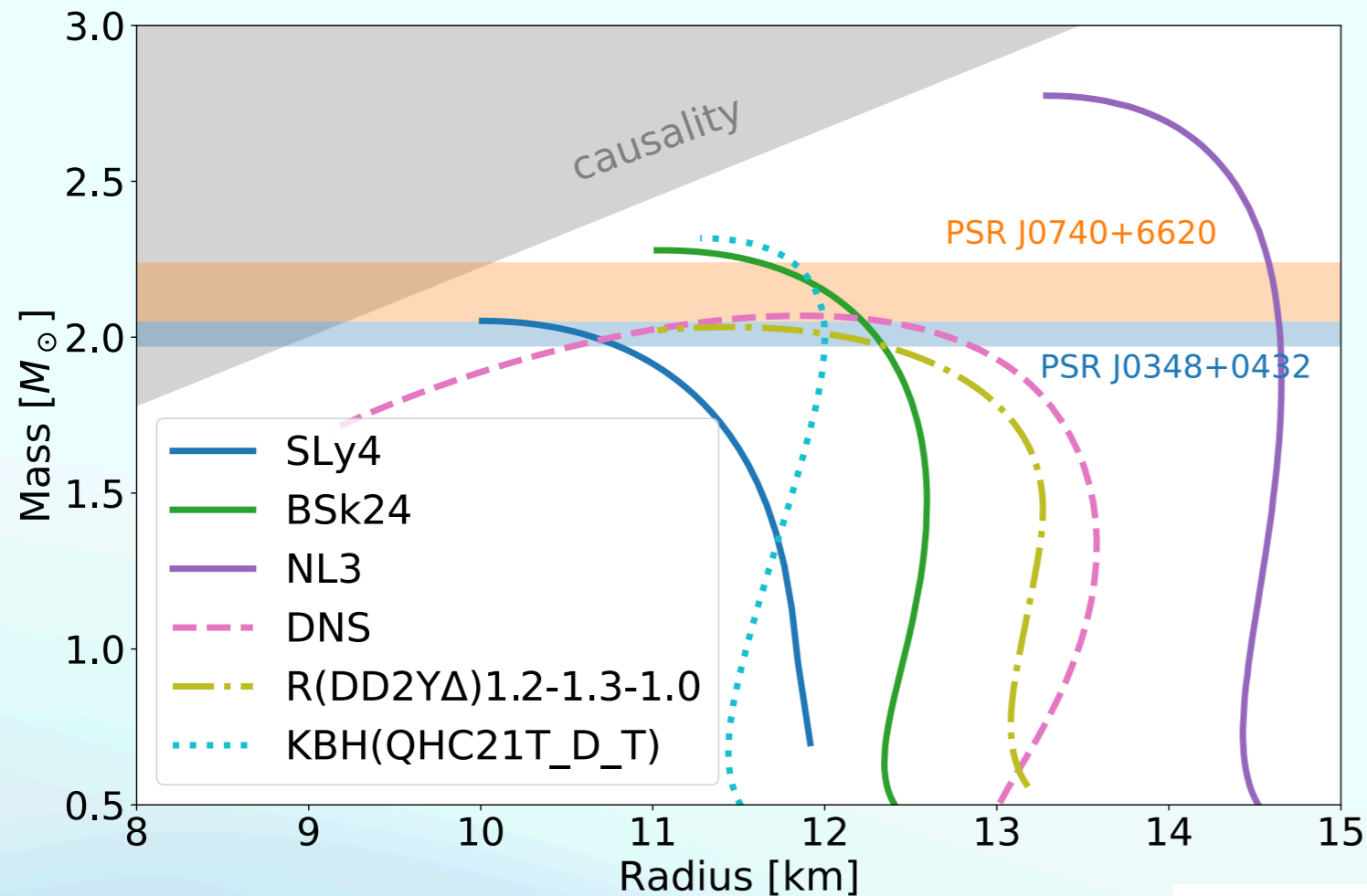
Introduction: Neutron Stars



- Generated after the gravitational collapse of the core of a massive star $M_{ZAMS} \sim 8 - 20/30 M_{\odot}$
- Compact objects: $1-2 M_{\odot}$ enclosed in a radius of 10-13 km
- Fast Rotation: $O(1 \text{ ms} - 10 \text{ s})$
- Strong Magnets: $O(10^8 - 10^{15} \text{ G})$

Introduction: Neutron Stars

Neutron Stars Mass-Radius relation



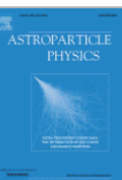
- Equation of State (EOS) unknown
- Different EOSs lead to different mass-radius relations
- Measuring the mass and the radius of NSs allow to identify the EOS
- This is easier in some systems with respect to others

SA, Graber & Rea 2024



Astroparticle Physics

Volume 158, June 2024, 102935

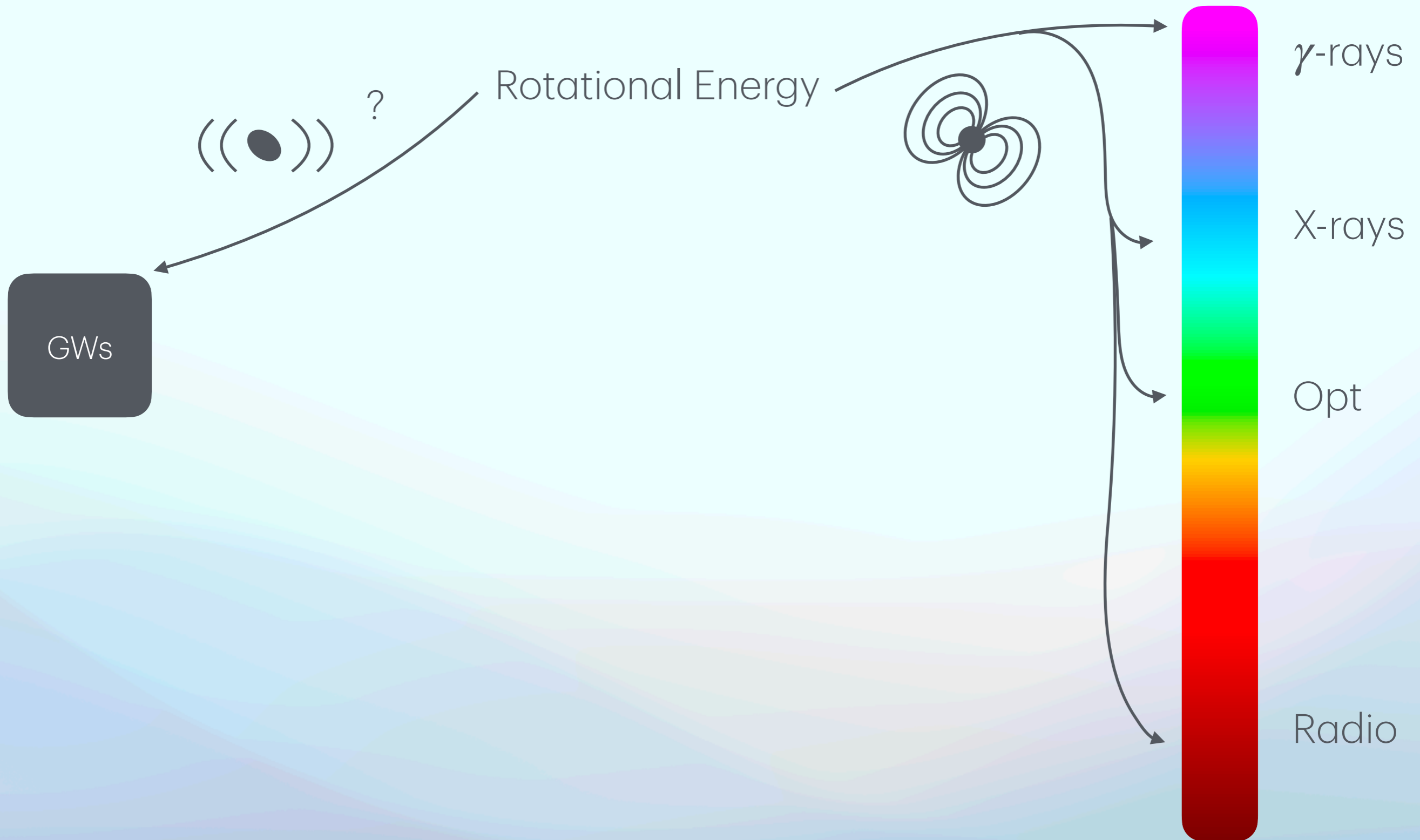


Neutron-star measurements in the multi-messenger Era

Stefano Ascenzi^{a b c 1}  , Vanessa Graber^{a b 1} , Nanda Rea^{a b} 

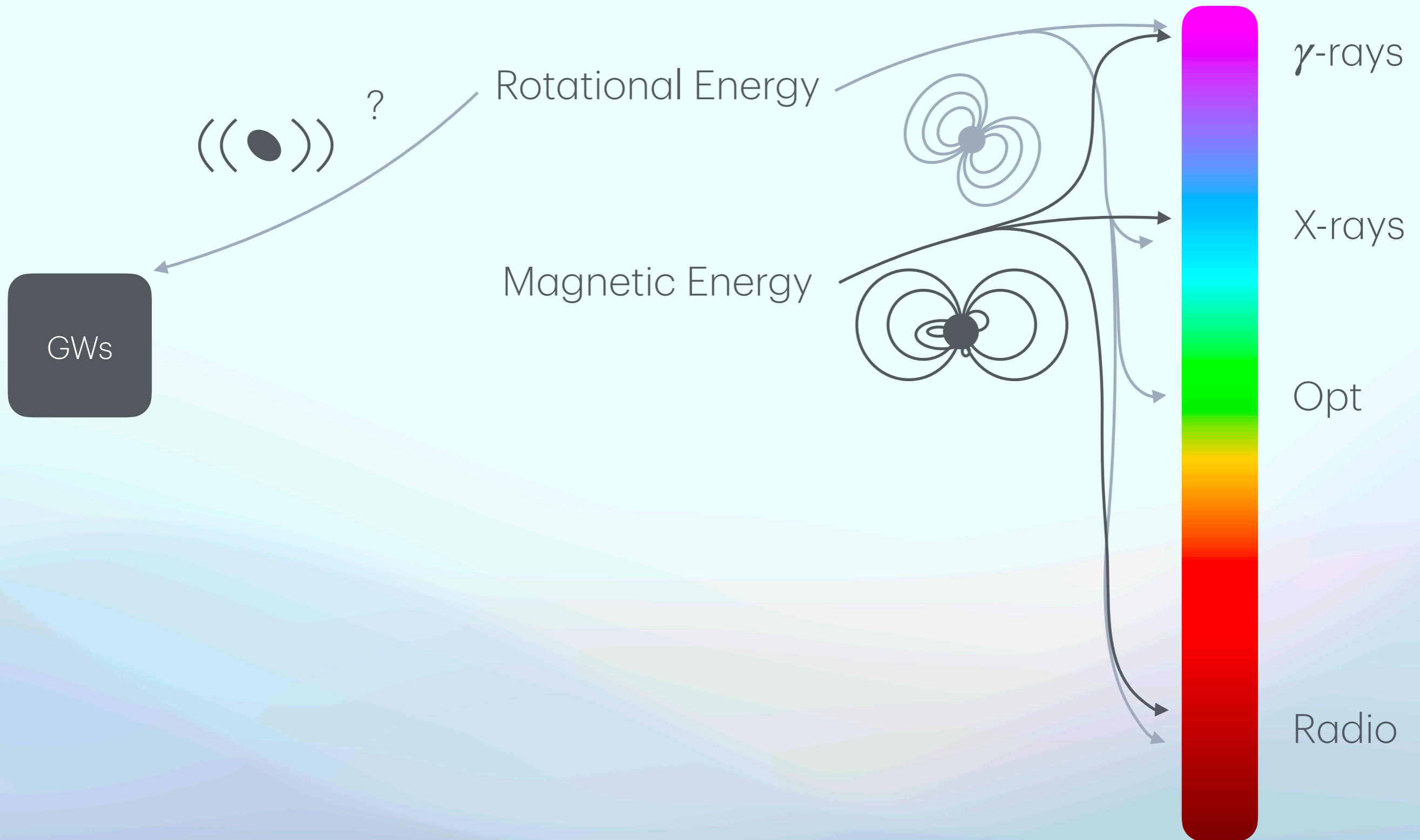
Introduction: How do/can we see Neutron Stars ?

Ultimate sources of energy for the emission of NSs



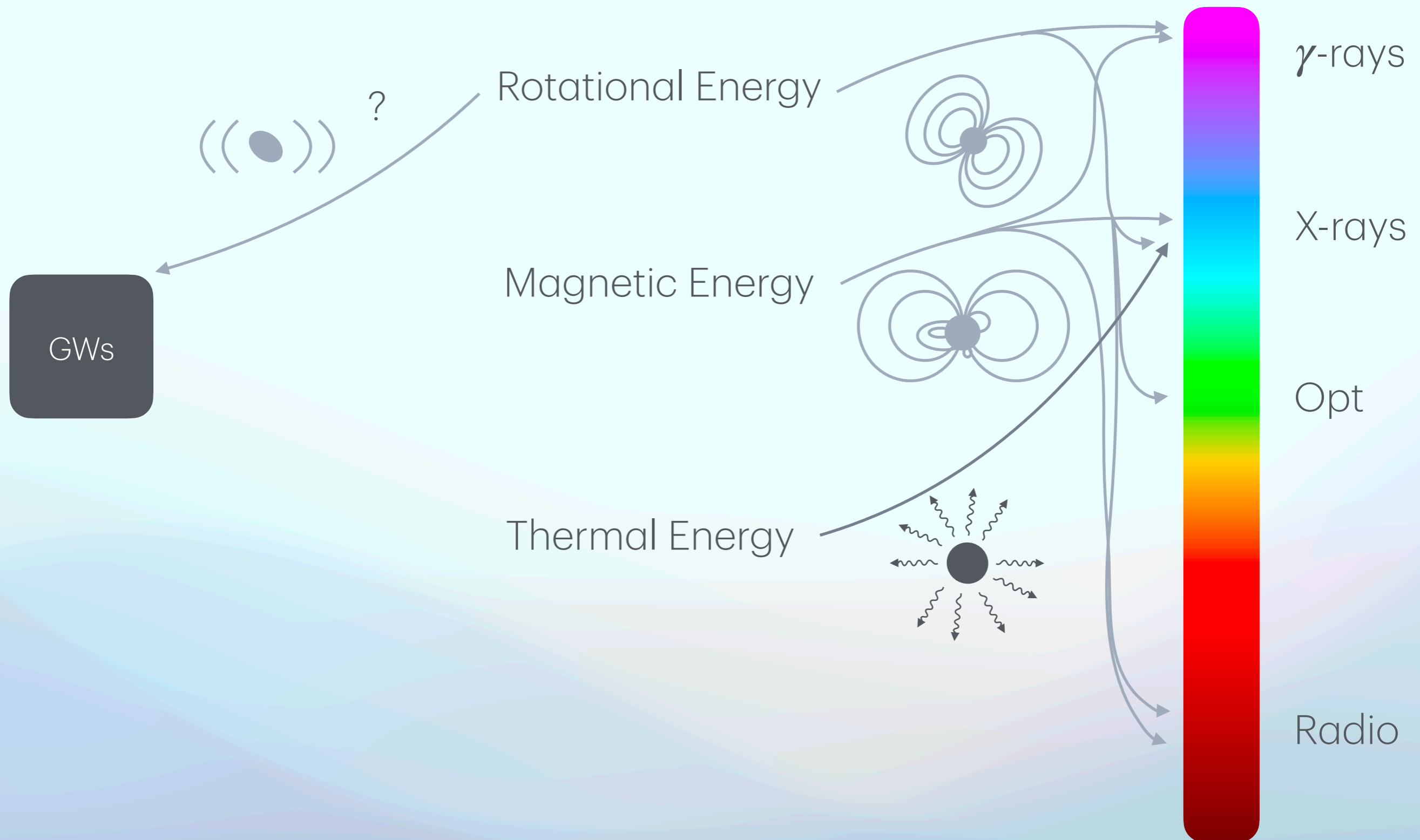
Introduction: How do/can we see Neutron Stars ?

Ultimate sources of energy for the emission of NSs



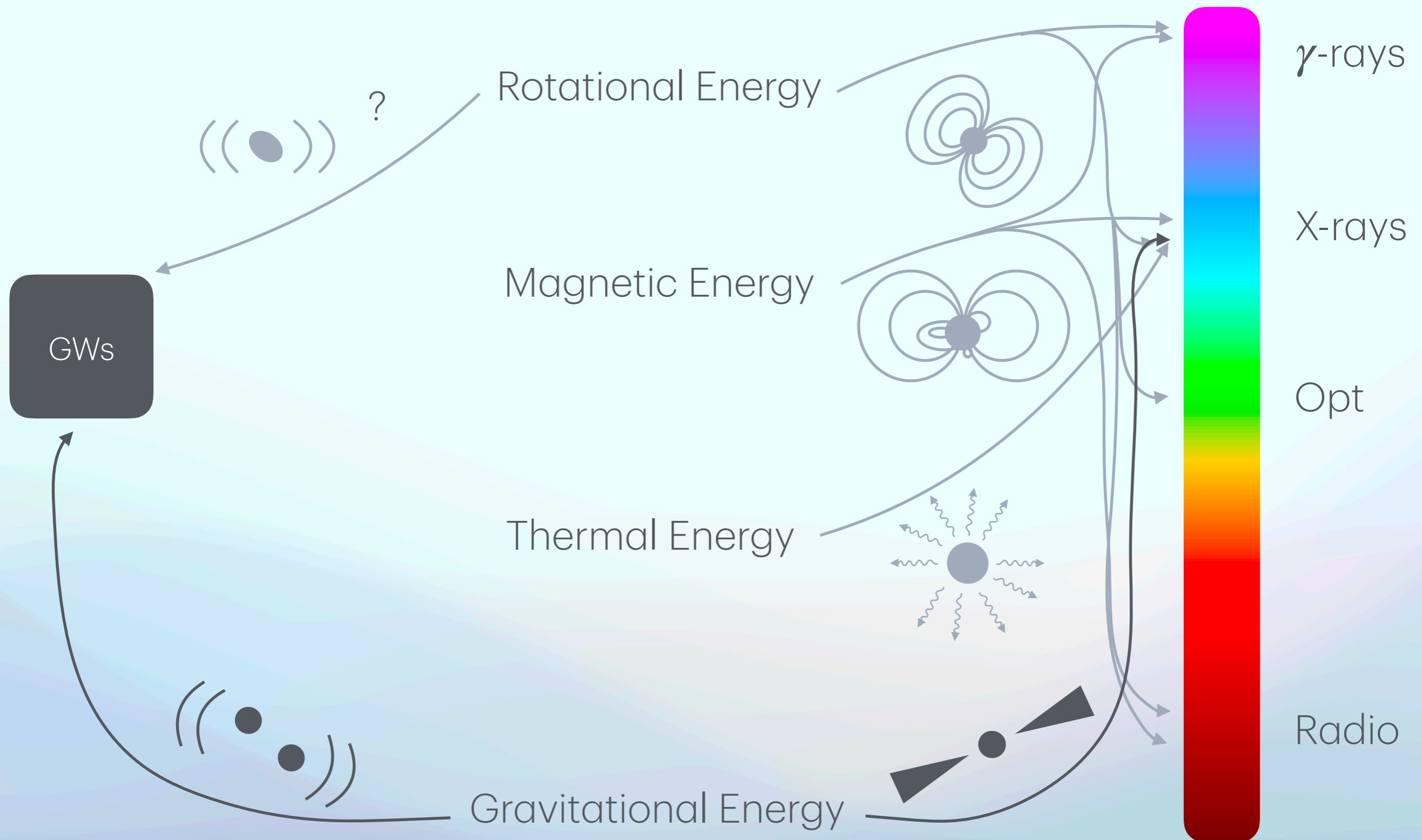
Introduction: How do/can we see Neutron Stars ?

Ultimate sources of energy for the emission of NSs

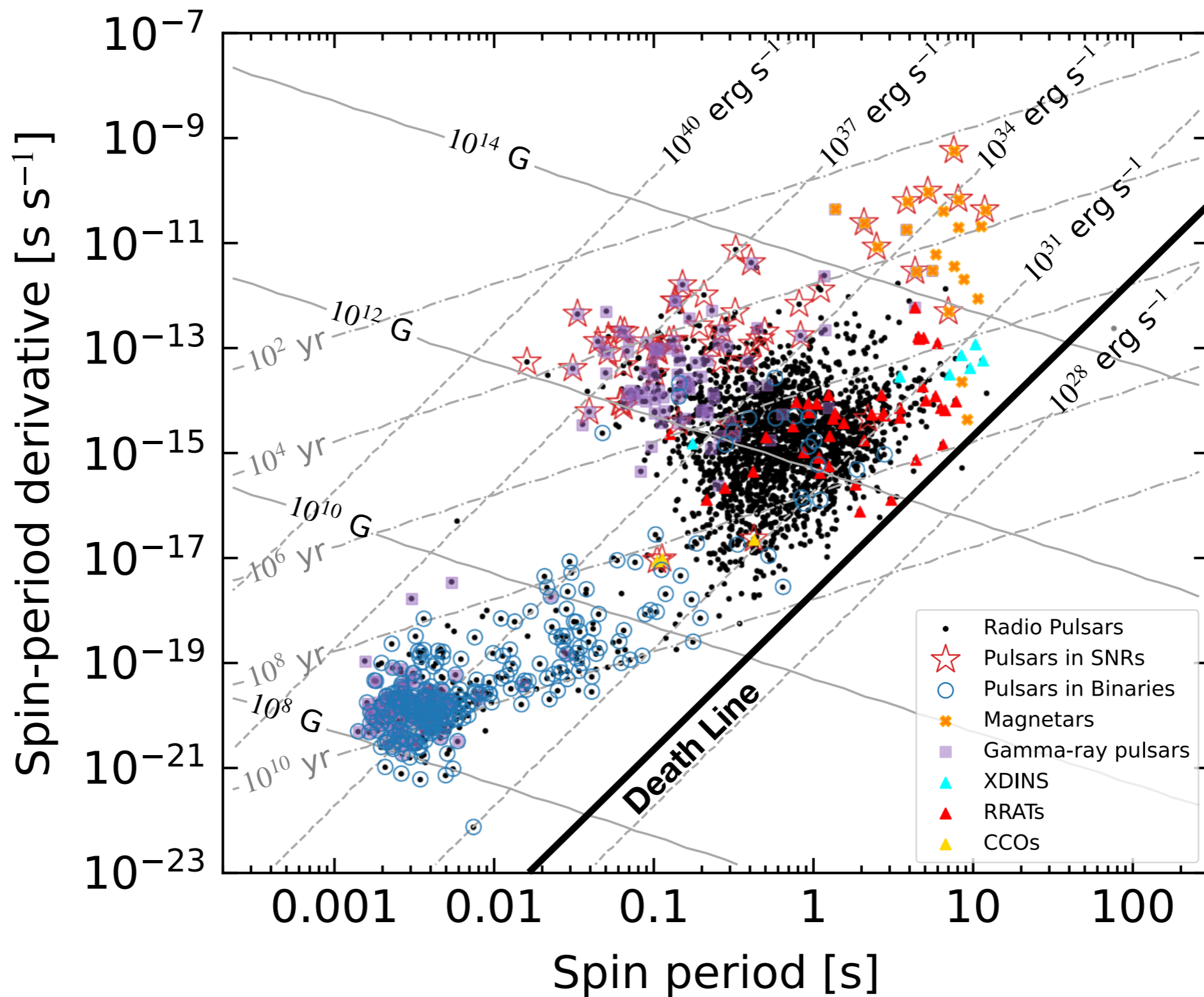


Introduction: How do/can we see Neutron Stars ?

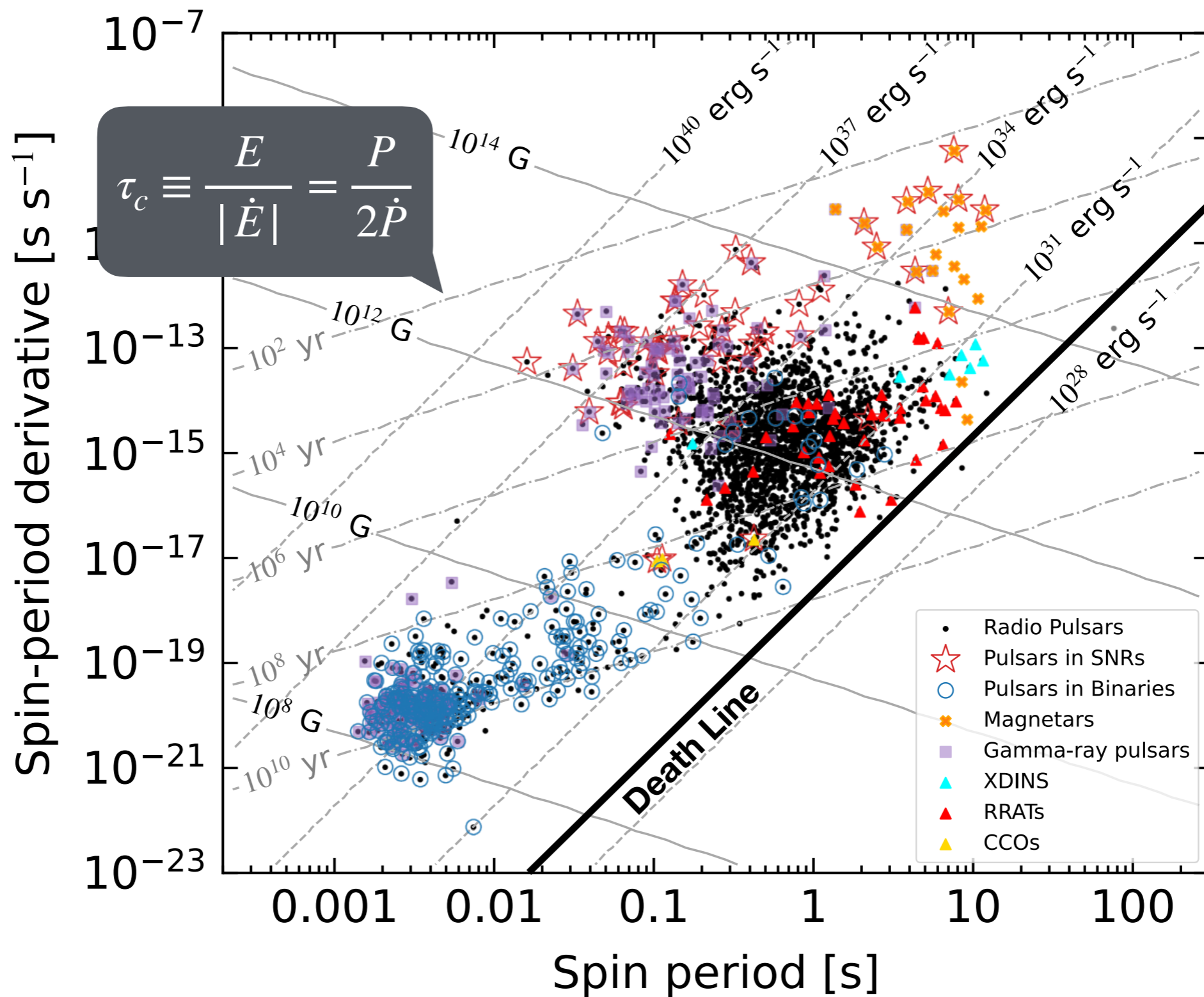
Ultimate sources of energy for the emission of NSs



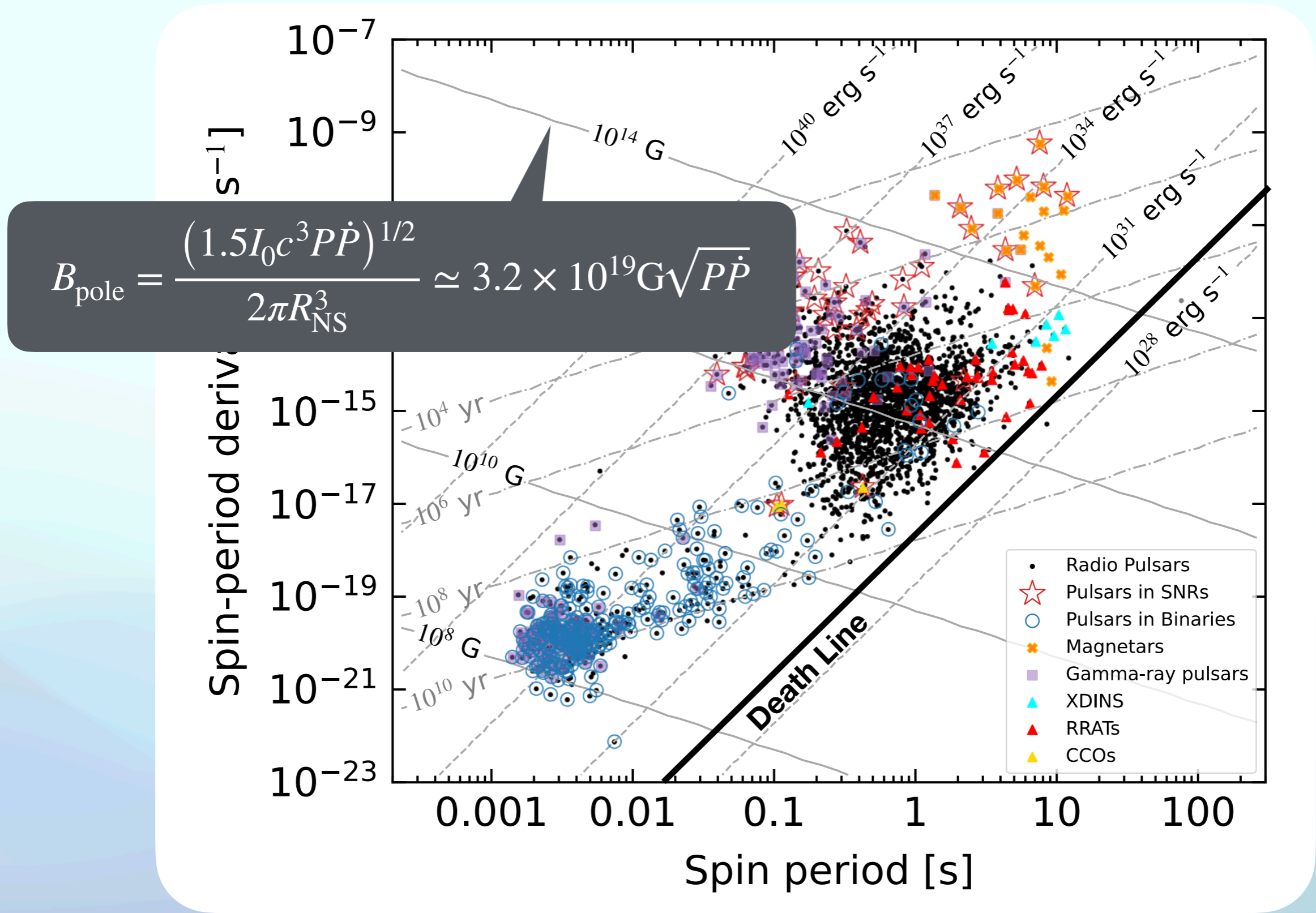
Introduction: $P - \dot{P}$ diagram



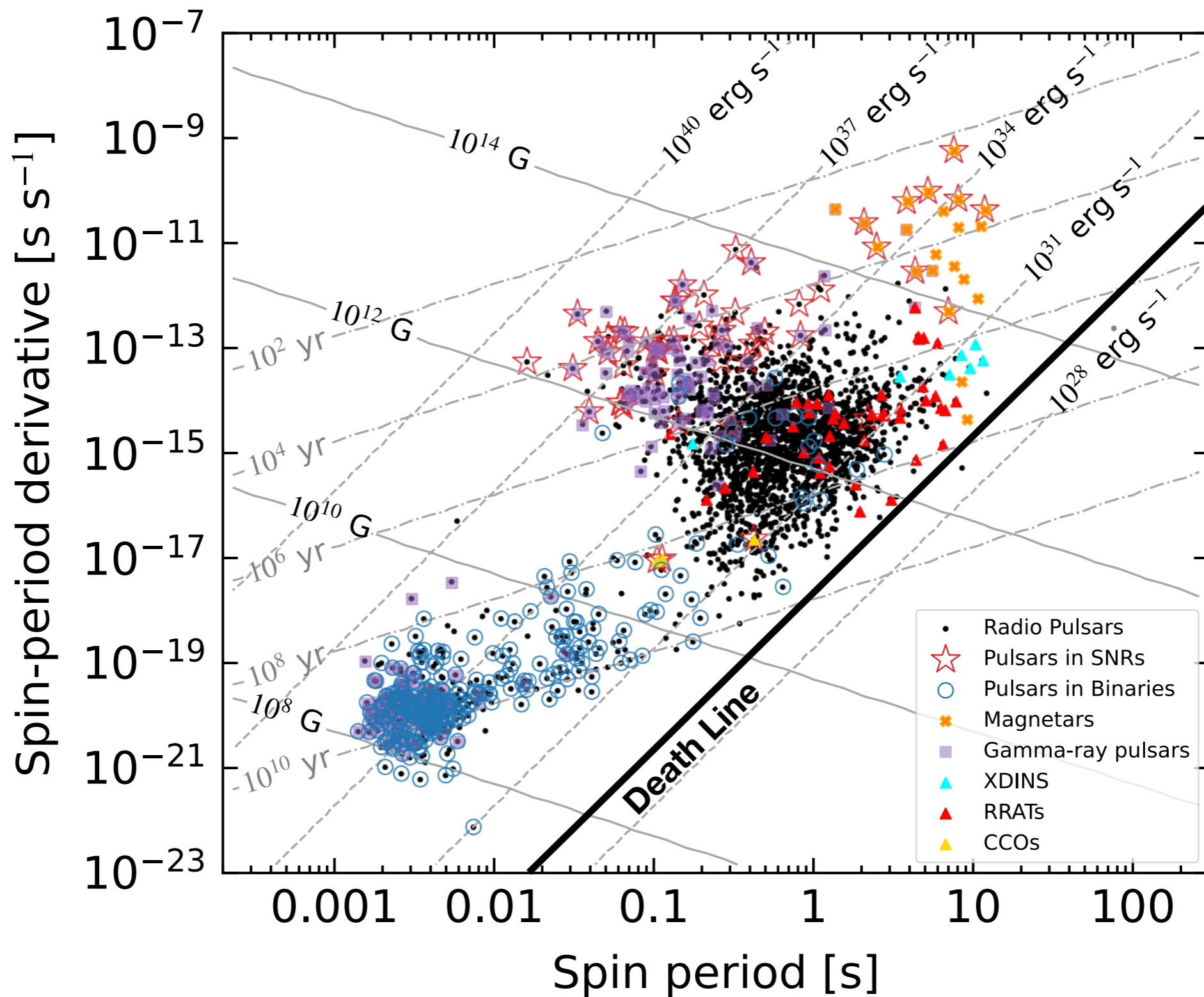
Introduction: $P - \dot{P}$ diagram



Introduction: $P - \dot{P}$ diagram



Introduction: $P - \dot{P}$ diagram



Rotational Powered Pulsars

Radio pulsars

Detection > 3300

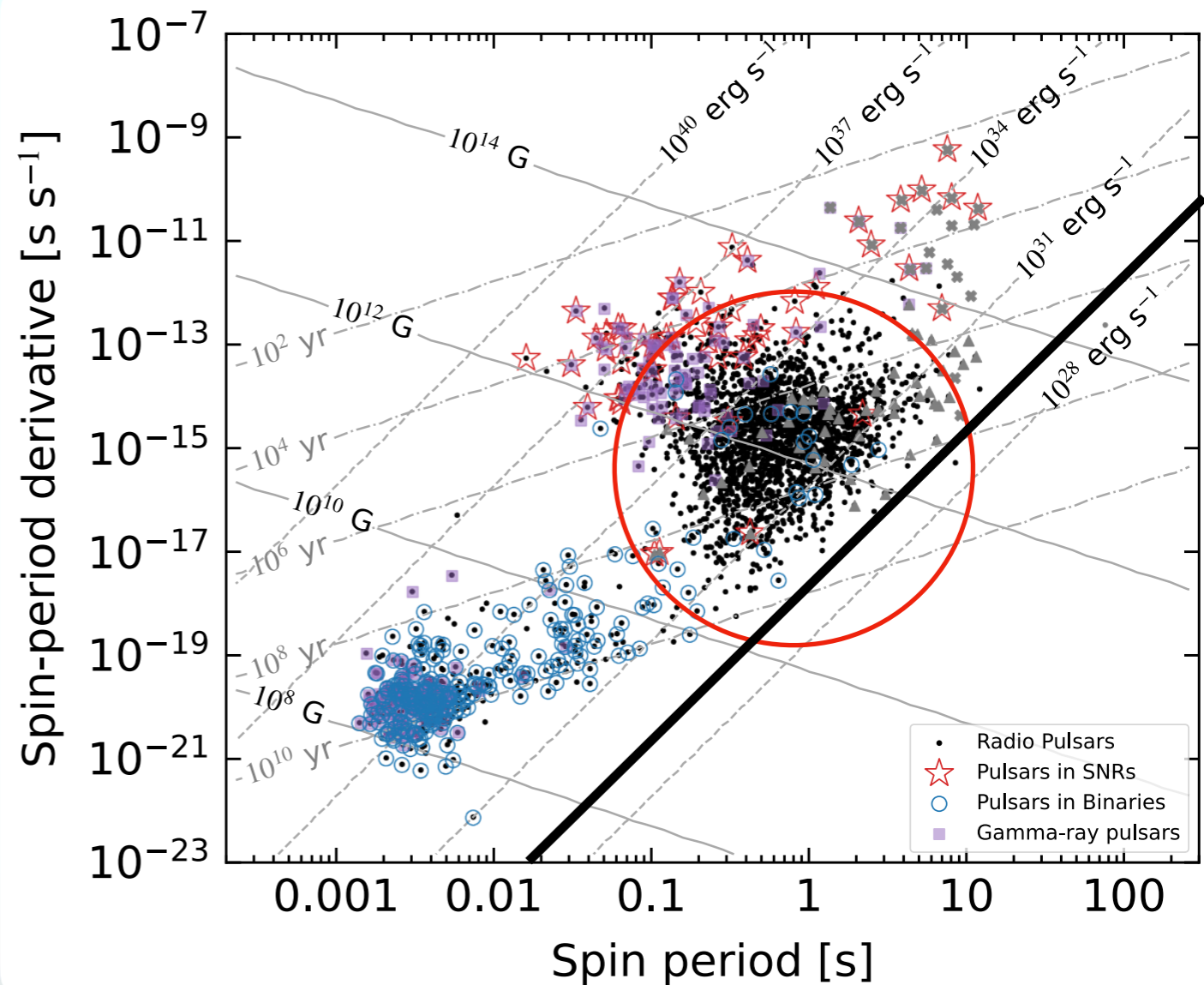
$L \ll \dot{E}_{\text{rot}}$ Powered by rotation

Slow radio pulsars

$P \sim 0.1 - 1$ s

$B \sim 10^{11} - 10^{13}$ G

$\tau_C \sim 10^3 - 10^8$ yr



Rotational Powered Pulsars

Millisecond Radio Pulsars

$$\dot{P} \sim 10^{-20} \text{ s/s}$$

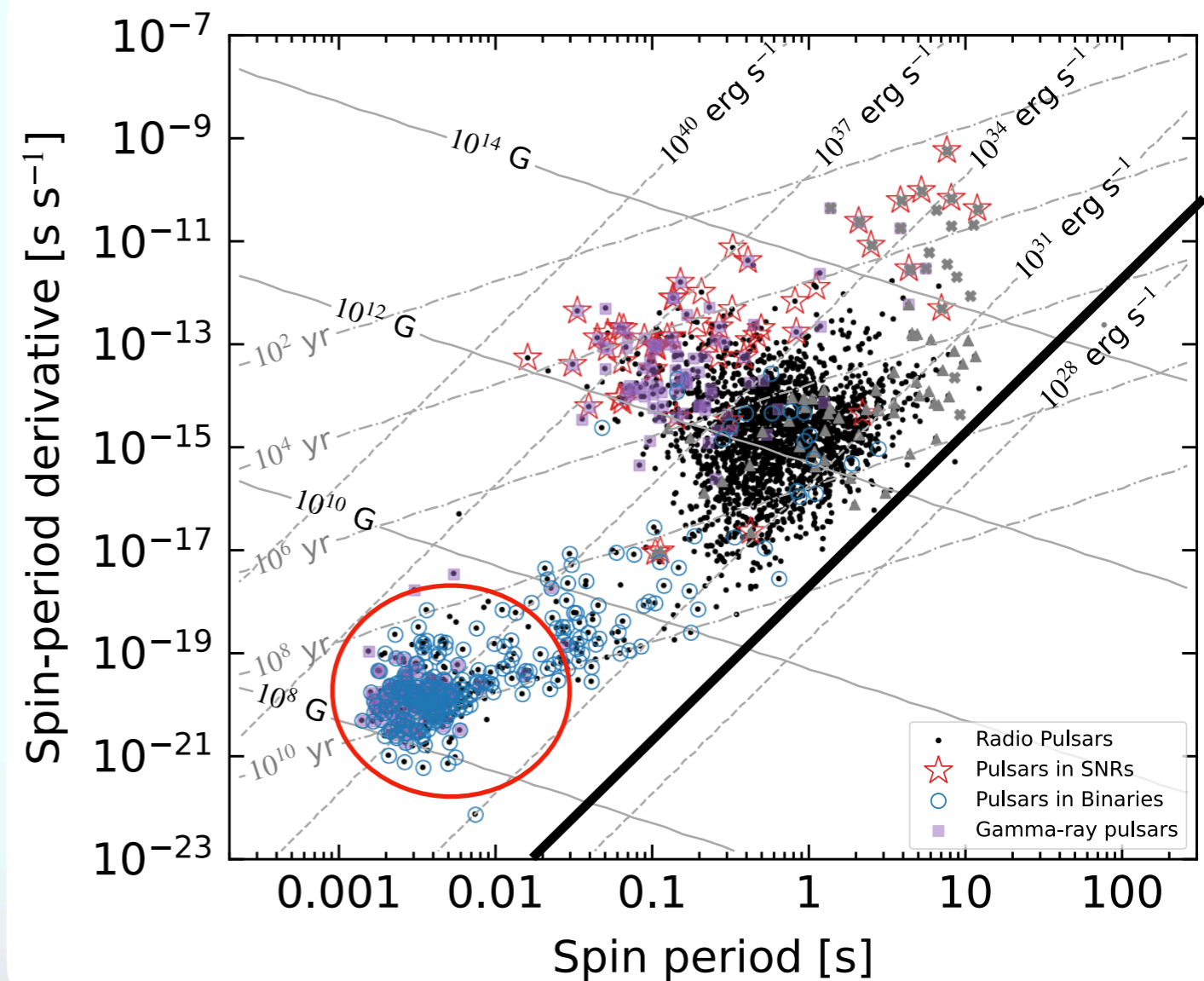
$$B \sim 10^8 \text{ G}$$

$$\tau_c \sim 10^{10} \text{ yrs}$$

671 detections ($P < 0.1 \text{ s}$)

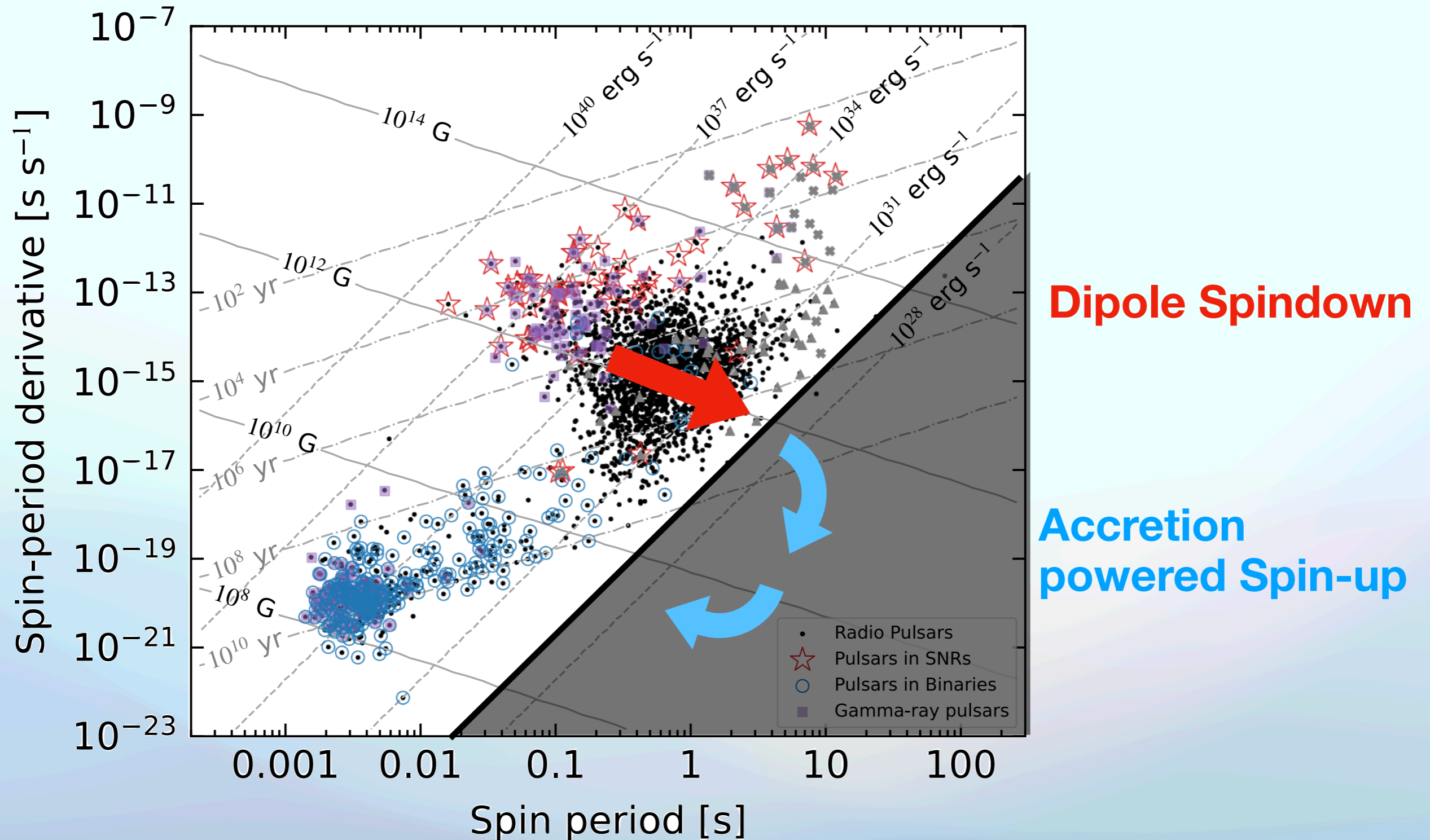
Extremely stable rotation

Very Accurate clocks



Rotational Powered Pulsars

Recycling Scenario



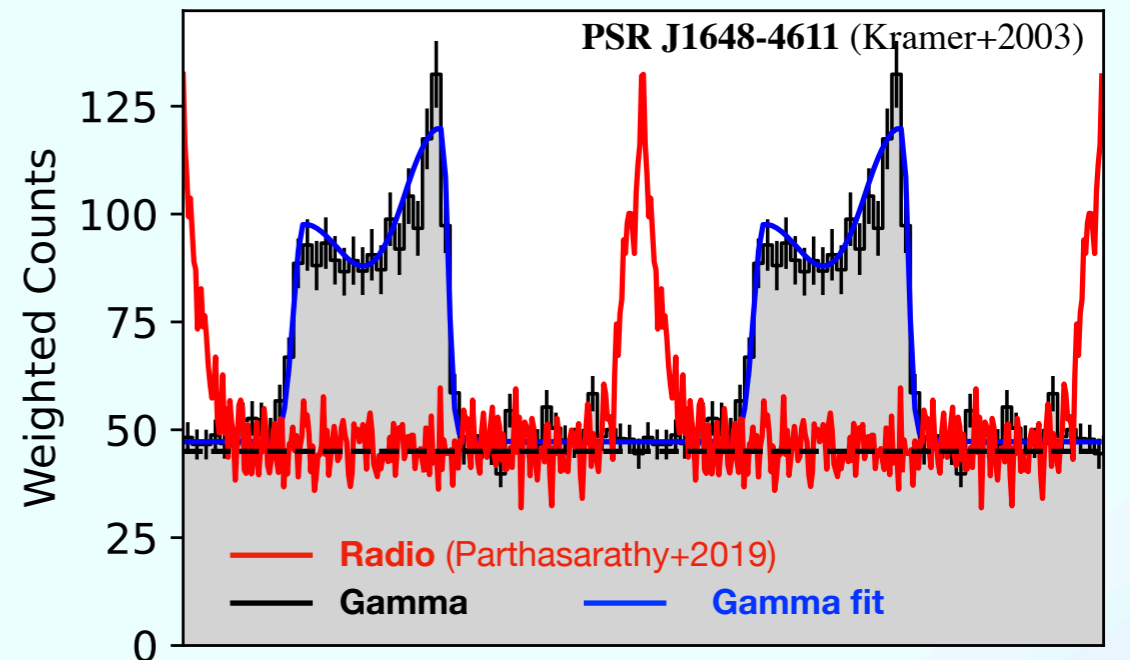
Rotational Powered Pulsars

Gamma-ray emission

Characteristic of the emission:

- $L_\gamma \propto \sqrt{\dot{E}}$
- Fraction of spindown power carried of by γ – ray
 $\sim 10^3$ times higher than that in radio
- Typically a double peak temporal profile
- Typically peaks not in phase with the radio peak

Pulsed profile



(Adapted from Smith+2023)

$$L_{\text{radio}}/\dot{E}_{\text{rot}} \sim 10^{-8} - 10^{-6}$$

$$L_{\text{X}}/\dot{E}_{\text{rot}} < 10^{-2} - 10^{-6}$$

$$L_\gamma/\dot{E}_{\text{rot}} \sim 10^{-1} - 10^{-3}$$

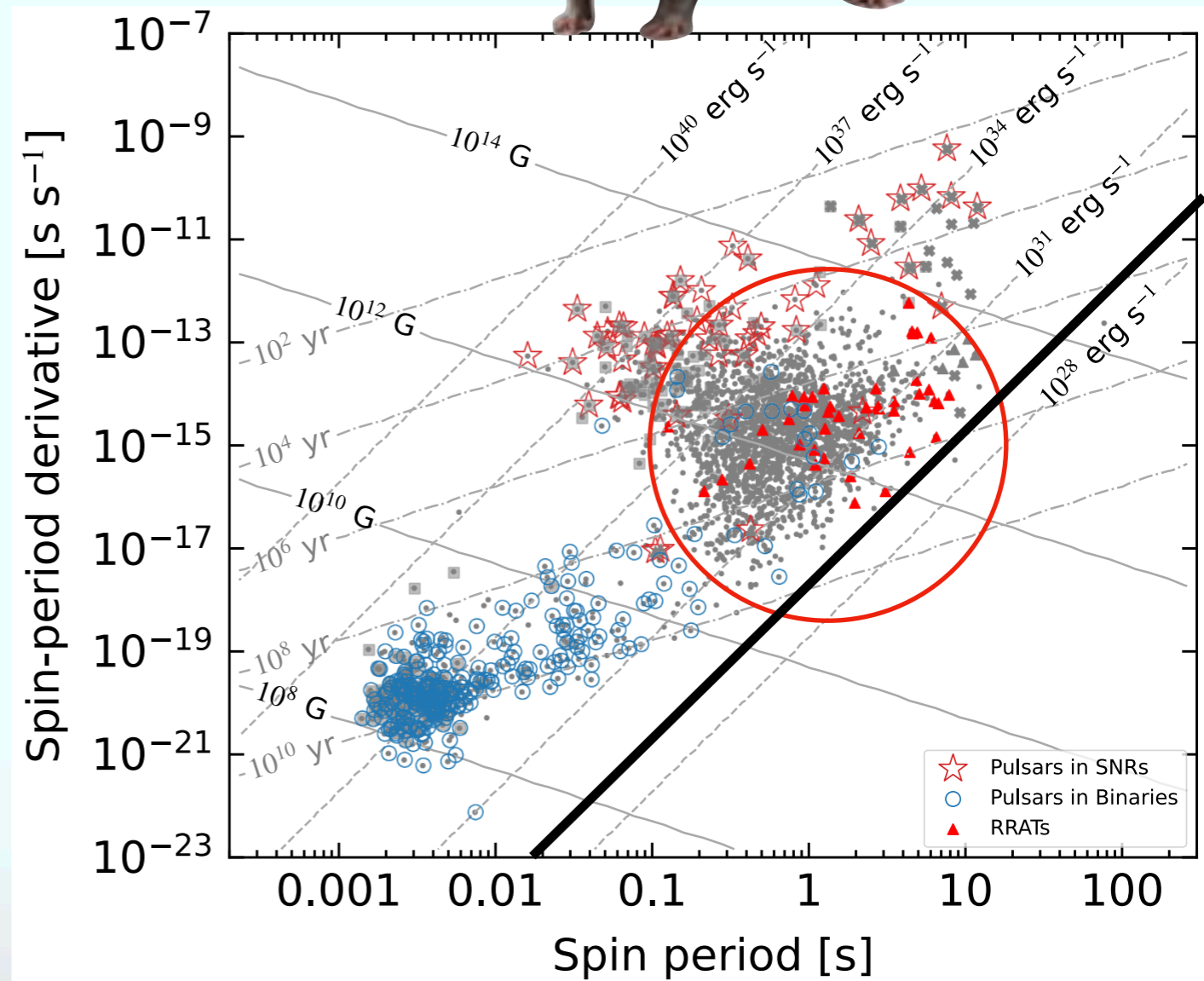
The RRATs: Rotational Radio Transient



Discovered as **bright** (0.1-3 Jy) short (2-30 ms) **radio bursts** that recurred randomly about every 4 min – 3 hr.

Discovery of periodicity. P measured for 2/3 and \dot{P} for 1/3 of them, over 115 detection.

Not a separate class of NS, but radio pulsars exhibiting extended switched off periods (nulling)



Magnetars

$$P \sim 1 - 12 \text{ s}$$

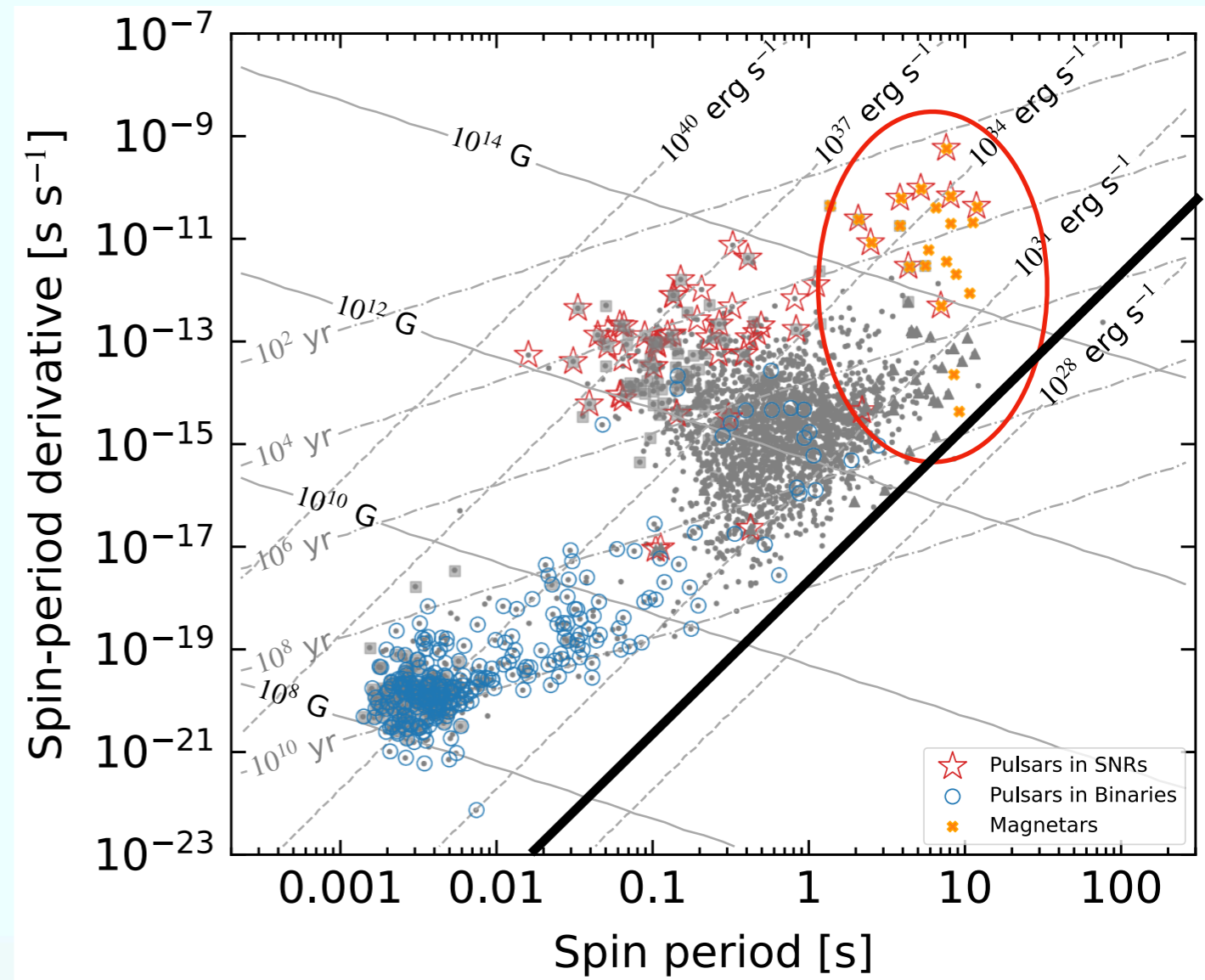
$$L_X \sim 10^{31} - 10^{36} \text{ erg/s}$$

$$B_{\text{dip}} \sim 10^{13} - 10^{15} \text{ G}$$

30 confirmed + 6 candidates

16 Soft Gamma-ray Repeaters (SGR; 12 confirmed, 4 candidates)

14 Anomalous X-ray Pulsars (AXPs; 12 confirmed, 2 candidates)

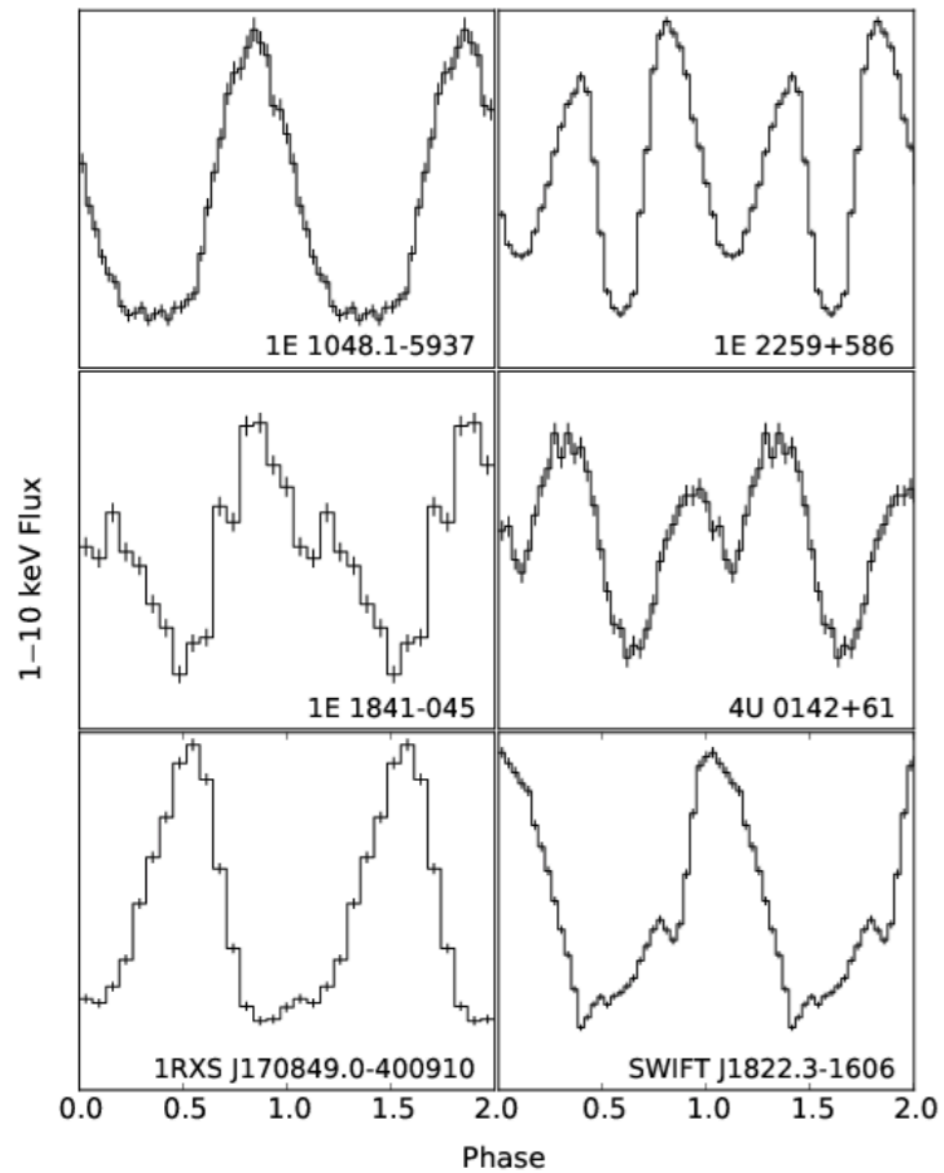


McGill Online Magnetar Catalog

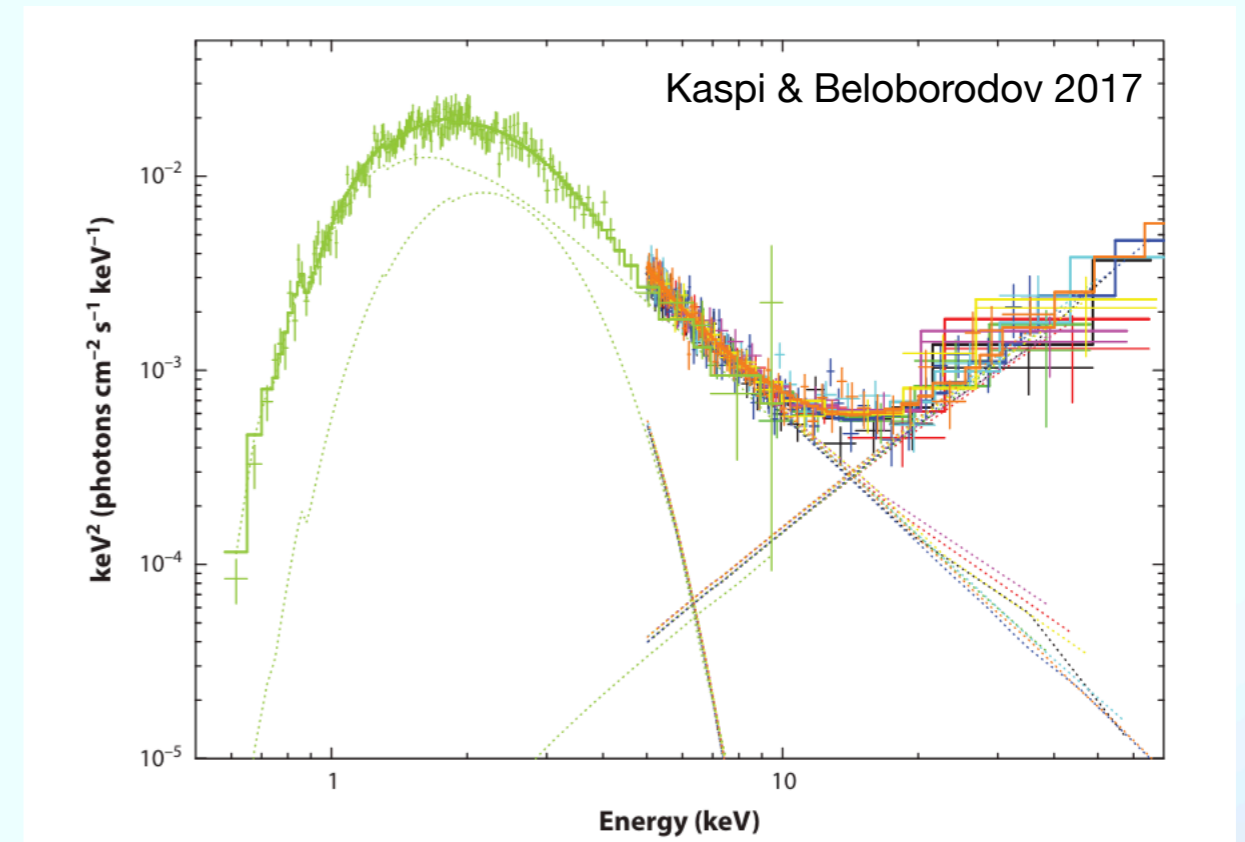
<http://www.physics.mcgill.ca/~pulsar/magnetar/main.html>

Magnetars

Lightcurves...



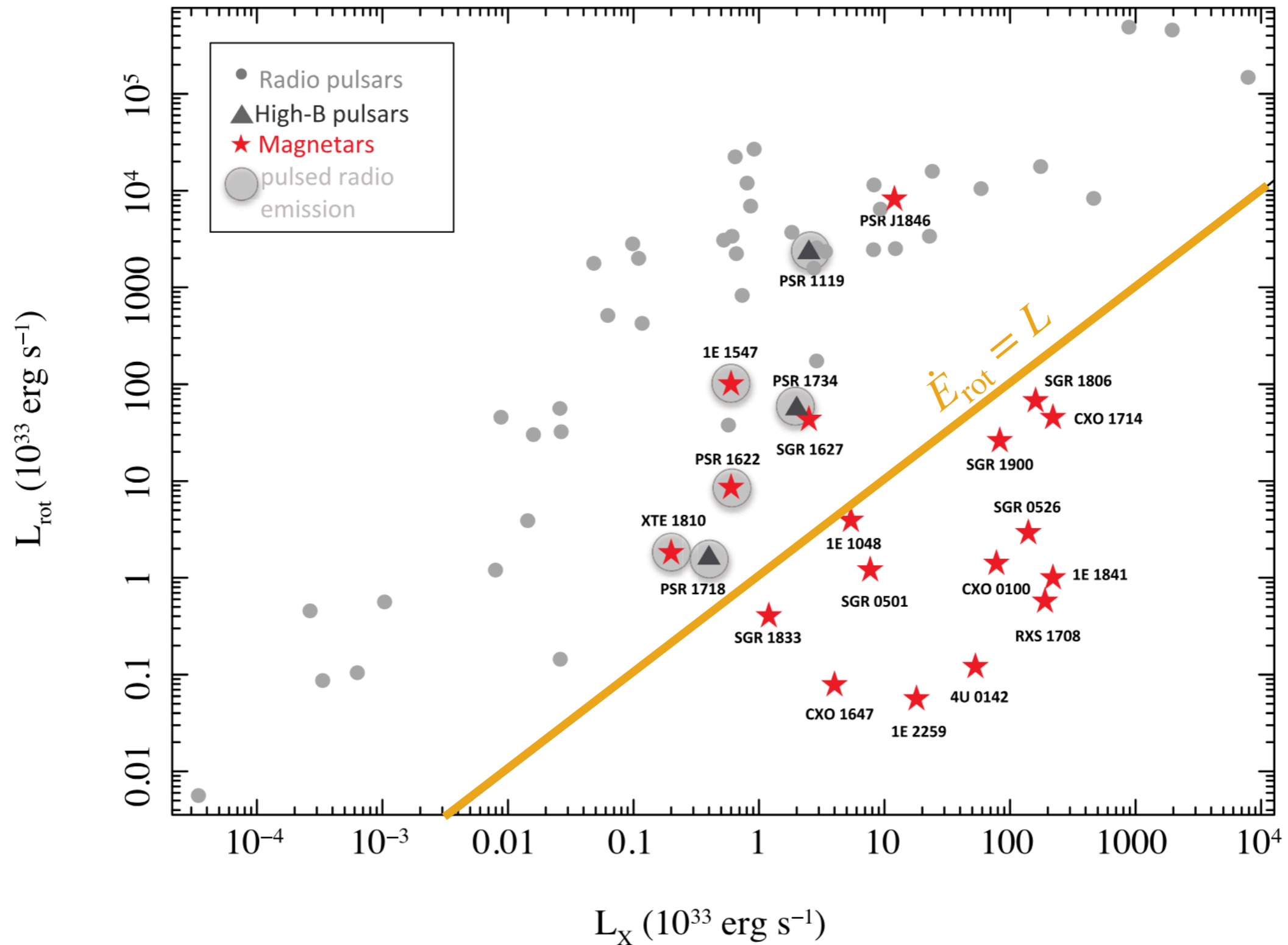
...and spectra



Kaspi & Beloborodov 2017

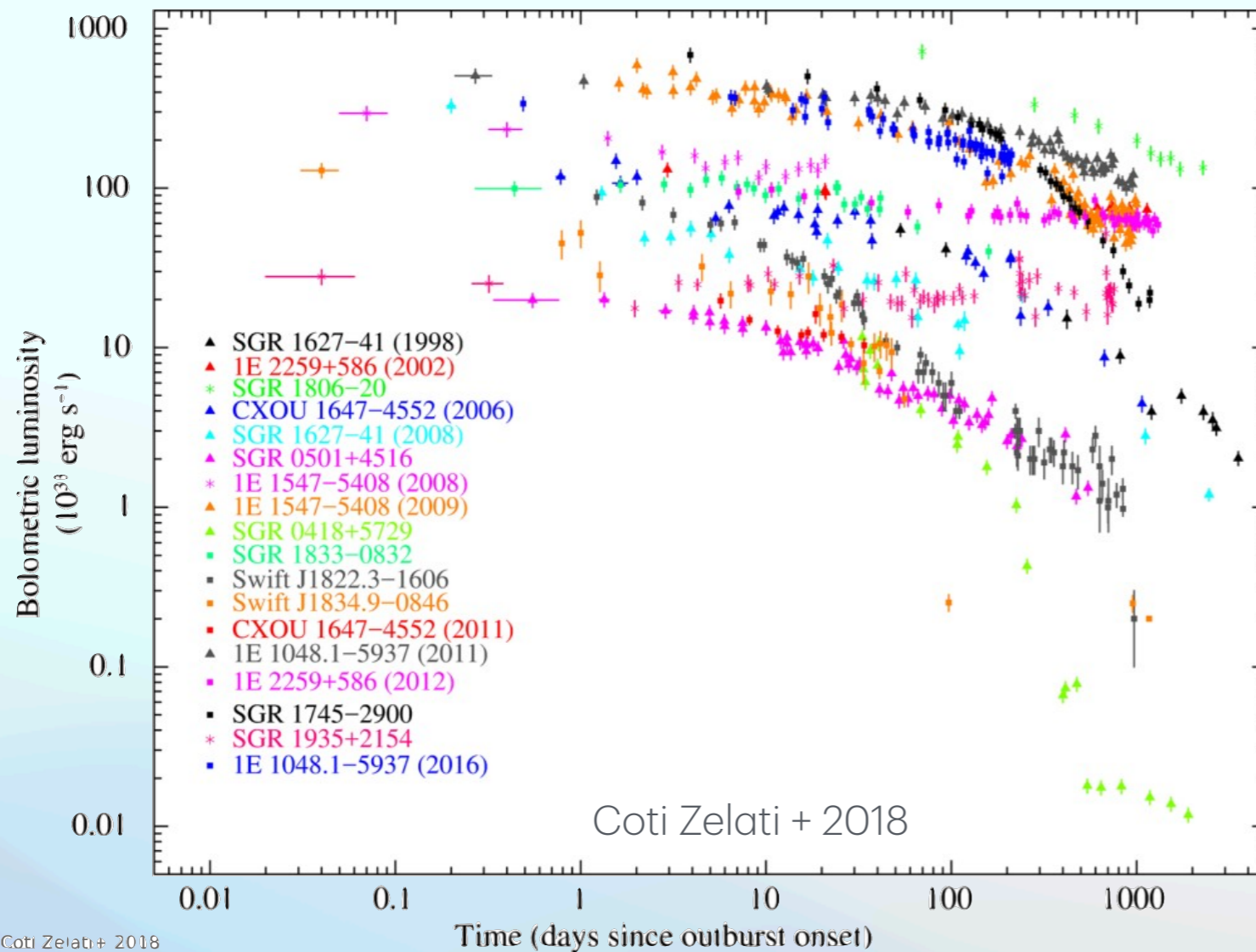
Magnetars

Rea 2013



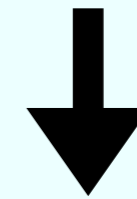
Magnetars

Transient activities: Outbursts



Coti Zelati+ 2018

Luminosity increased up to 3 orders of magnitudes. Lower quiescent luminosity, larger increase.



Saturation luminosity at $\sim 10^{36} \text{ erg/s}$

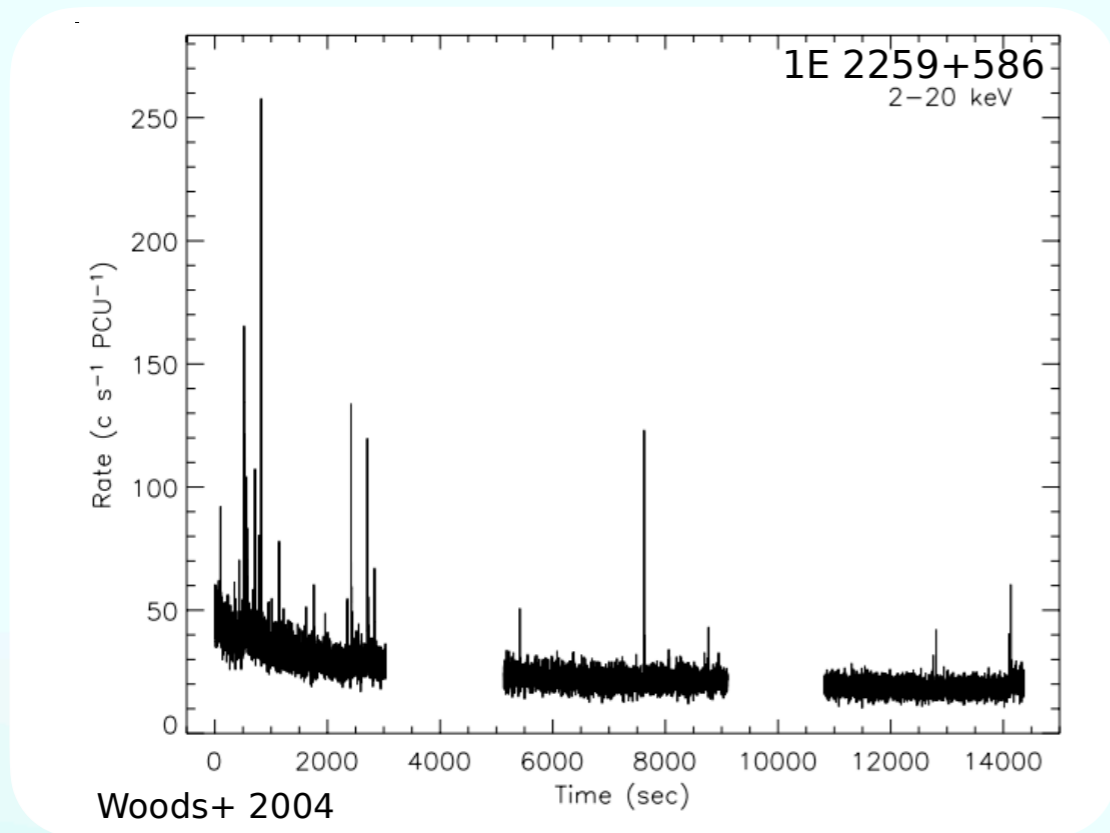
P and \dot{P} changes irregularly with glitches and anti-glitches



<http://magnetars.ice.csic.es/#/welcome>

Magnetars

Transient activity



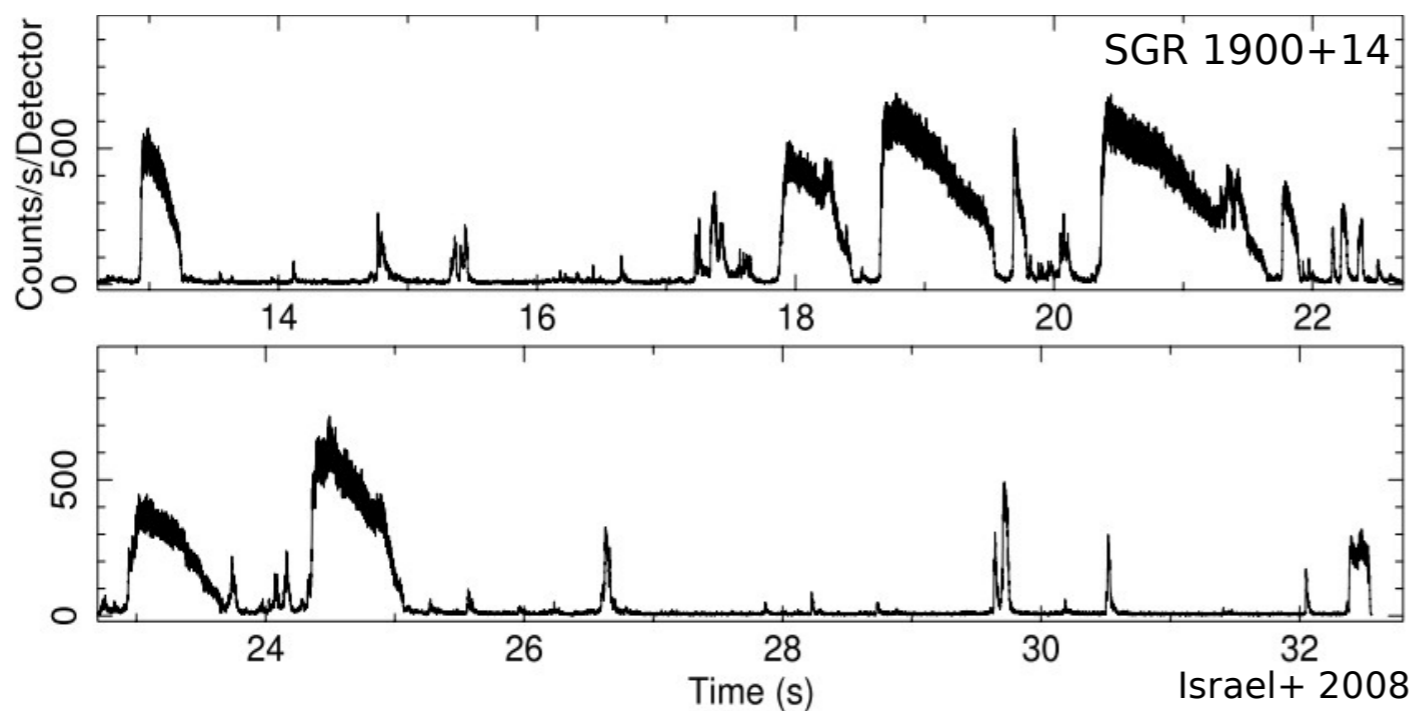
Short Bursts

Duration ~ 0.01-1 s

$L_{\text{peak}} \sim 10^{39} - 10^{41}$ erg/s

Sporadically or storm

Thermal Spectra



Intermediate Bursts

Duration ~ 1-40 s

$L_{\text{peak}} \sim 10^{41} - 10^{43}$ erg/s

Abrupt onset

Thermal Spectra

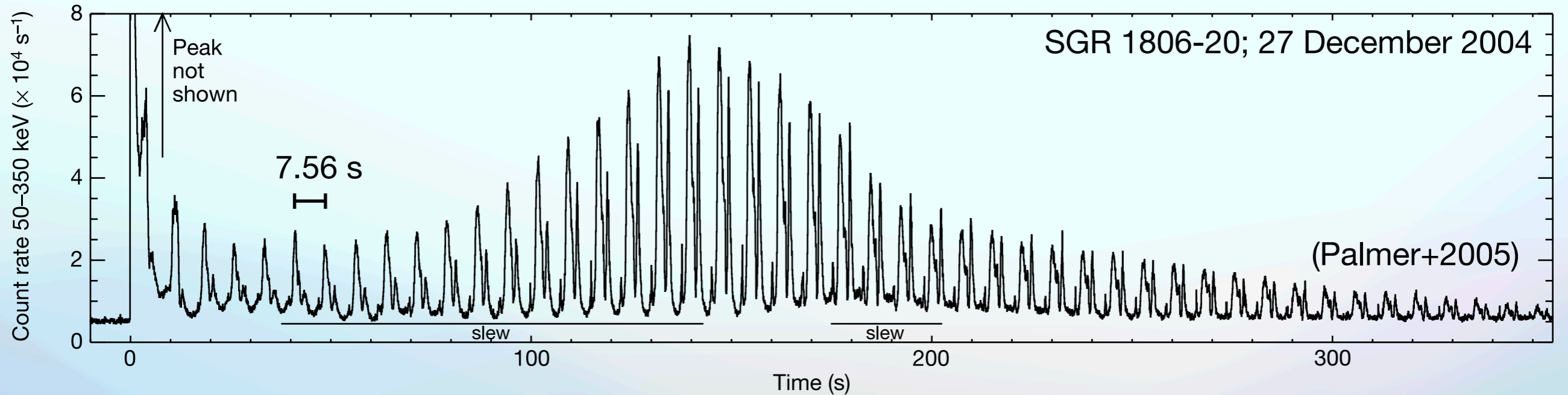
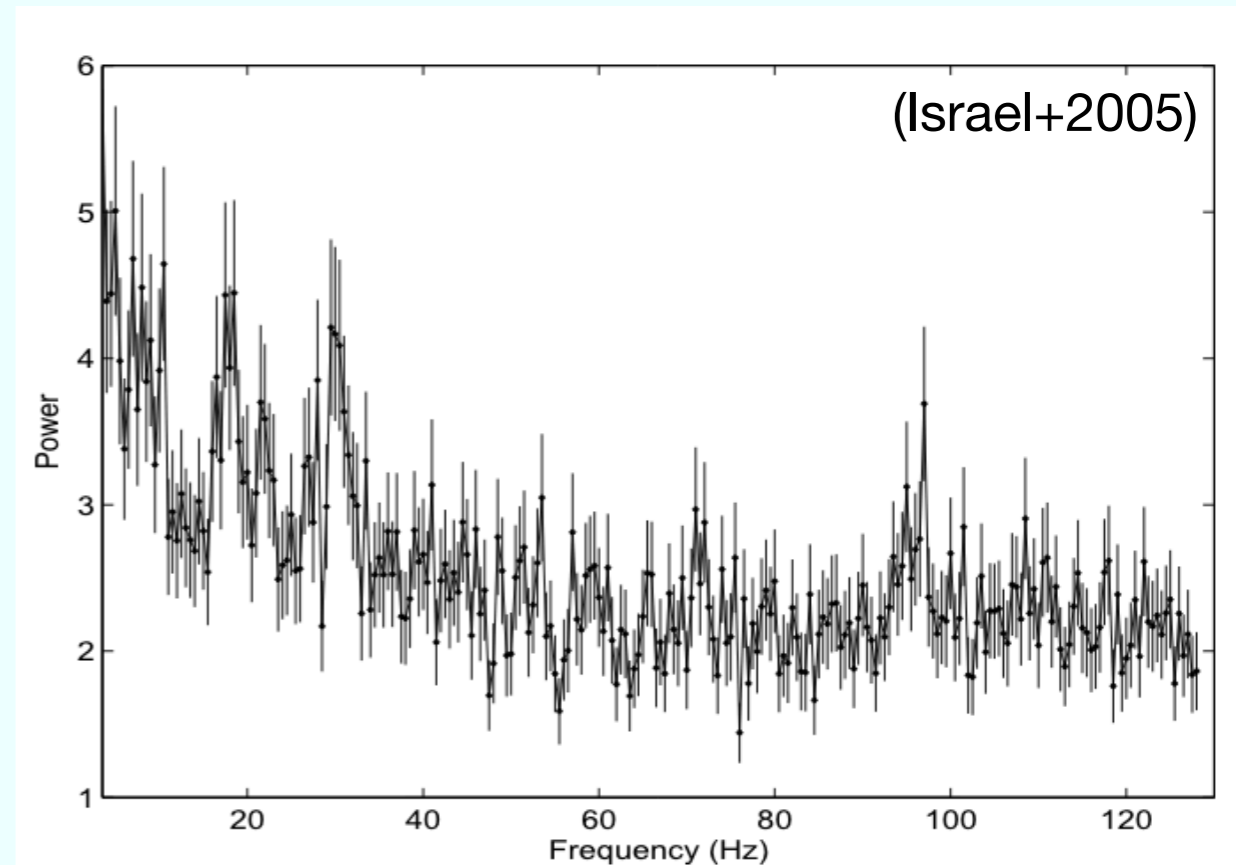
Magnetars

Transient activities: Giant Flares

Luminosity $L_X > 10^{44}$ erg/s

Short-Hard
Spike

Softer Pulsating Tail



X-ray Dim Isolated Neutron Stars (XDINSs)

Distance $\lesssim 500$ pc

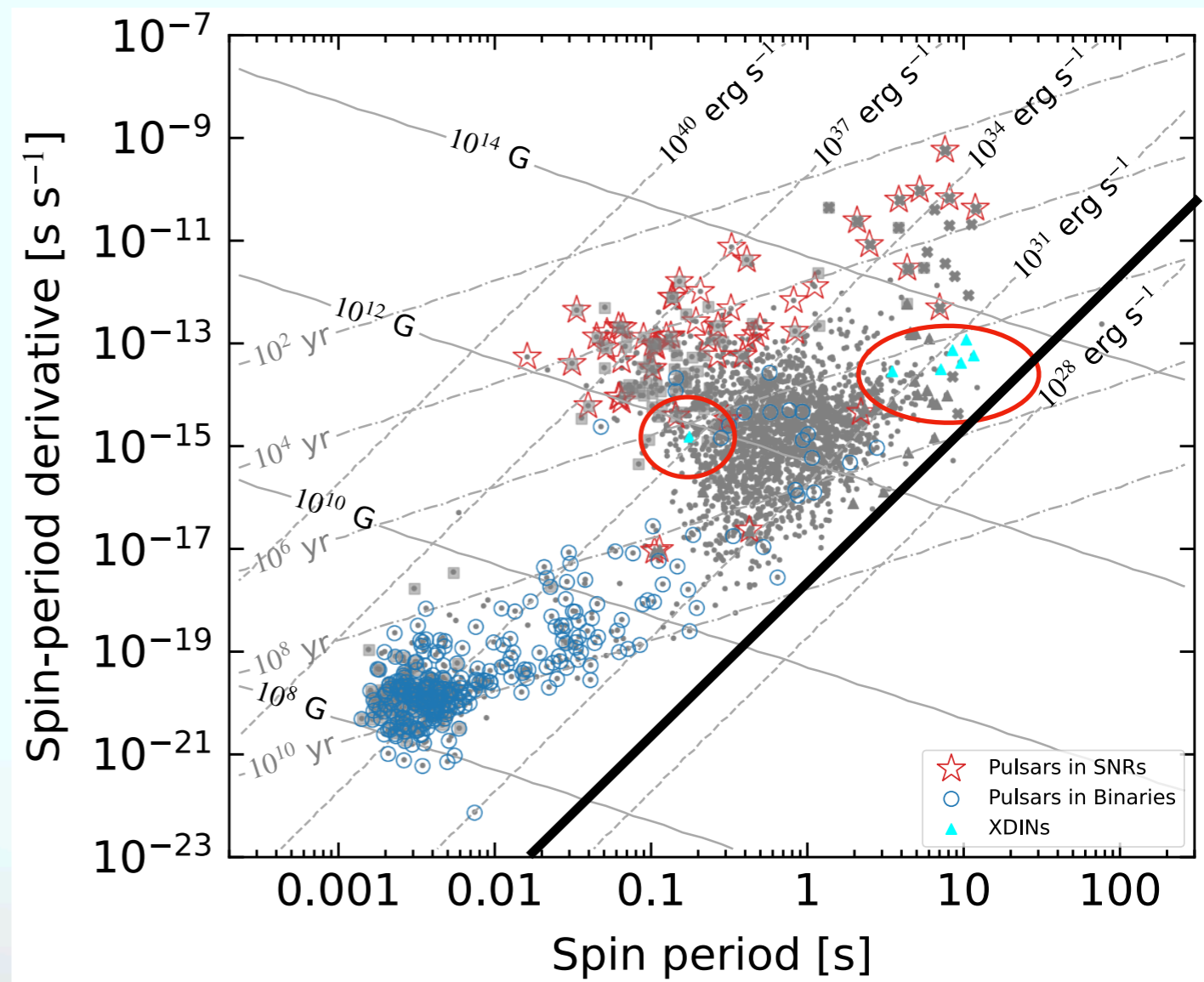
Spin period: $P \sim 3 - 11$ s

Age: $\tau \sim 10^6$ yr

Luminosity: $L_X \sim 10^{31-32}$ erg/s

No radio emission

Faint optical emission with respect to X-ray

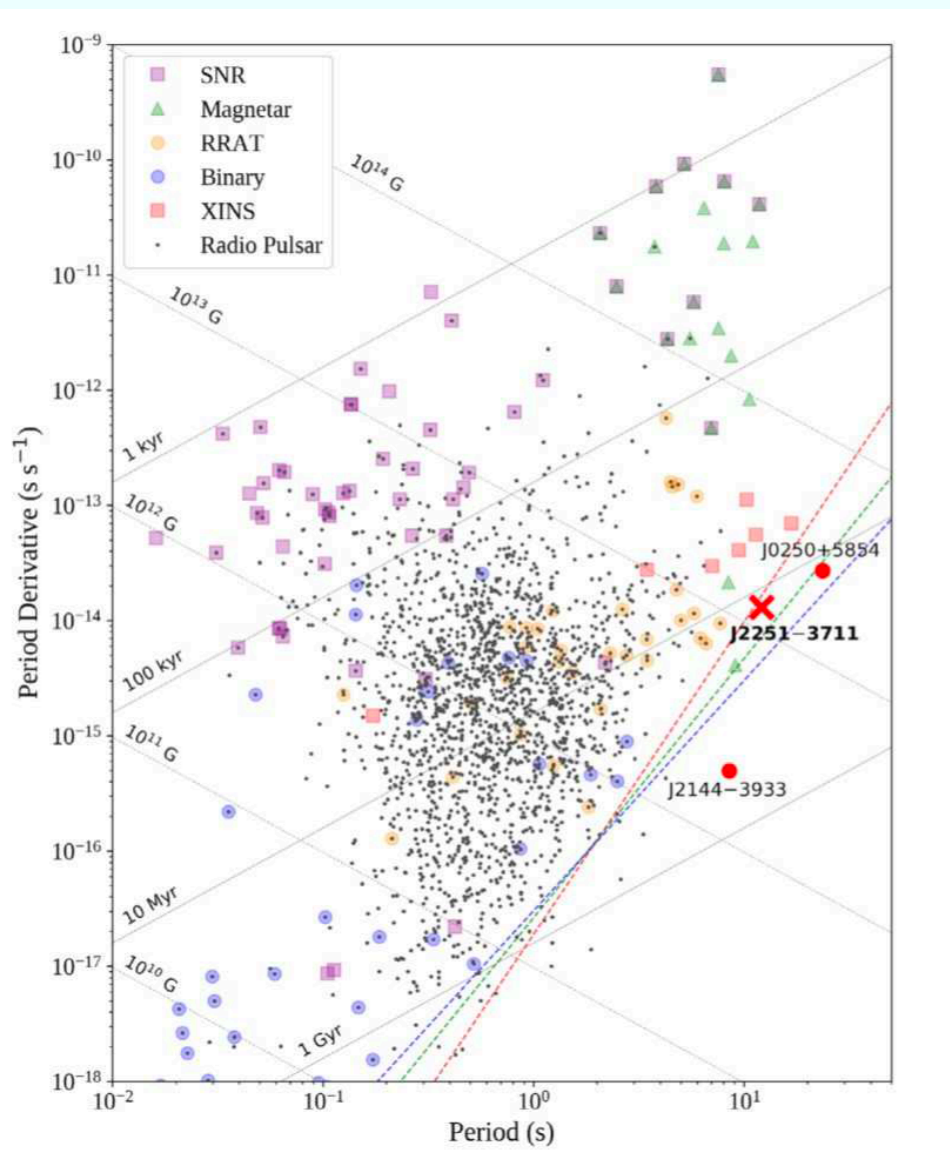


Peculiar Cases

Slow pulsars

Similar spin characteristic to the low-B magnetars and the XDINSs

Young+1999; Tan+2018; Morello+ 2020

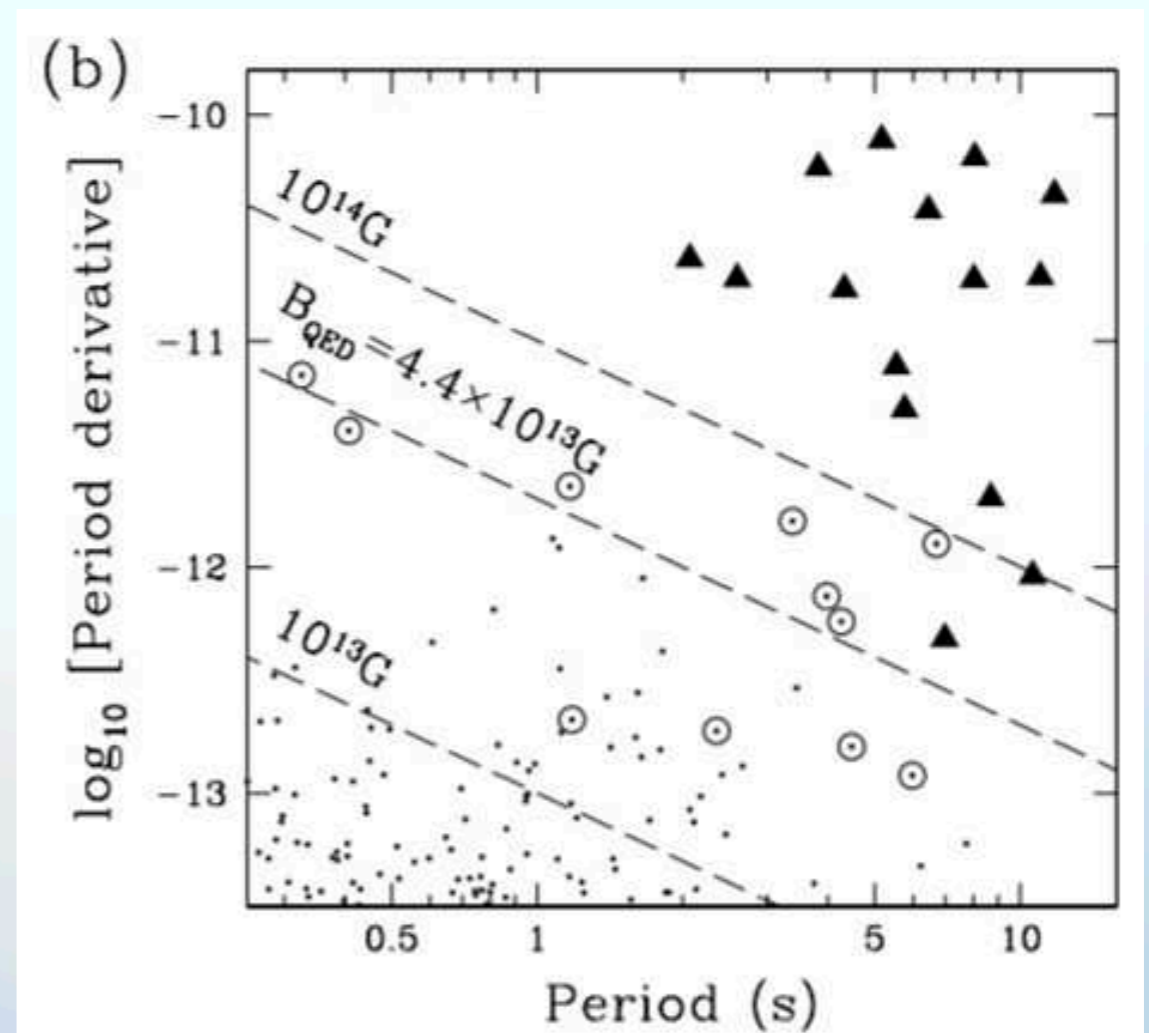


Morello+ 2020

High-B pulsars

Spin parameters similar to this of the magnetars, implying comparable field intensity $B > 10^{13} \text{ G}$

Two them show magnetar-like activity



Courtesy of Alice Borghese

Ng & Kaspi 2011

Central Compact Objects (CCOs)

Point-like X-ray sources close to the center of supernova remnants (SNR)

No optical-radio counterpart

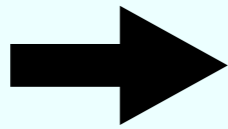
A dozen of sources, 3 period spin period measured

Thermal-like spectrum $k_B T_{BB} \sim 0.1$ keV

$$L_X \sim 10^{33} \text{ erg/s}$$

$$P \sim 0.1 \text{ s}$$

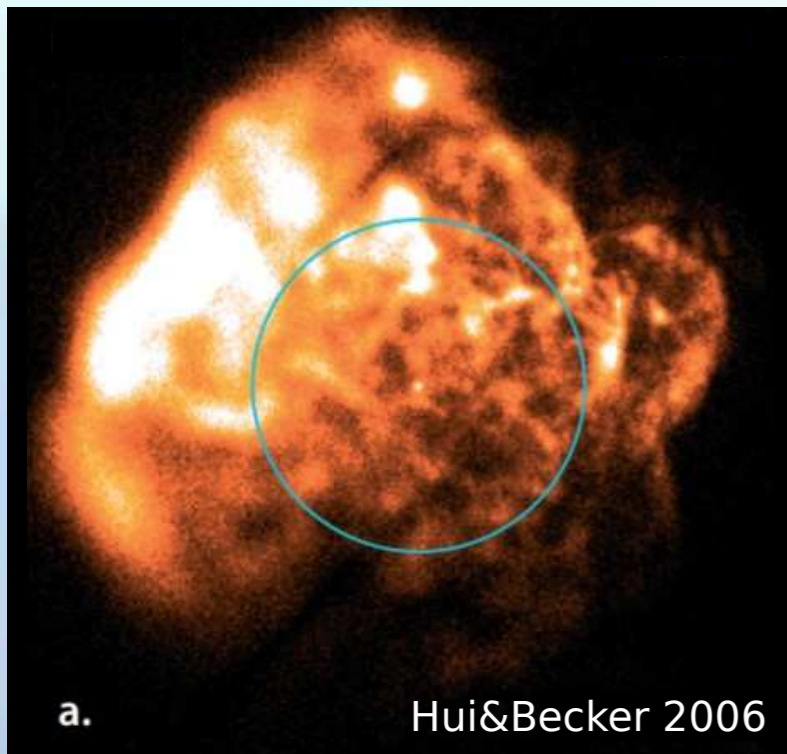
$$\dot{P} \sim 10^{-17} \text{ s s}^{-1}$$



$$B \sim 10^{10} - 10^{11} \text{ G}$$

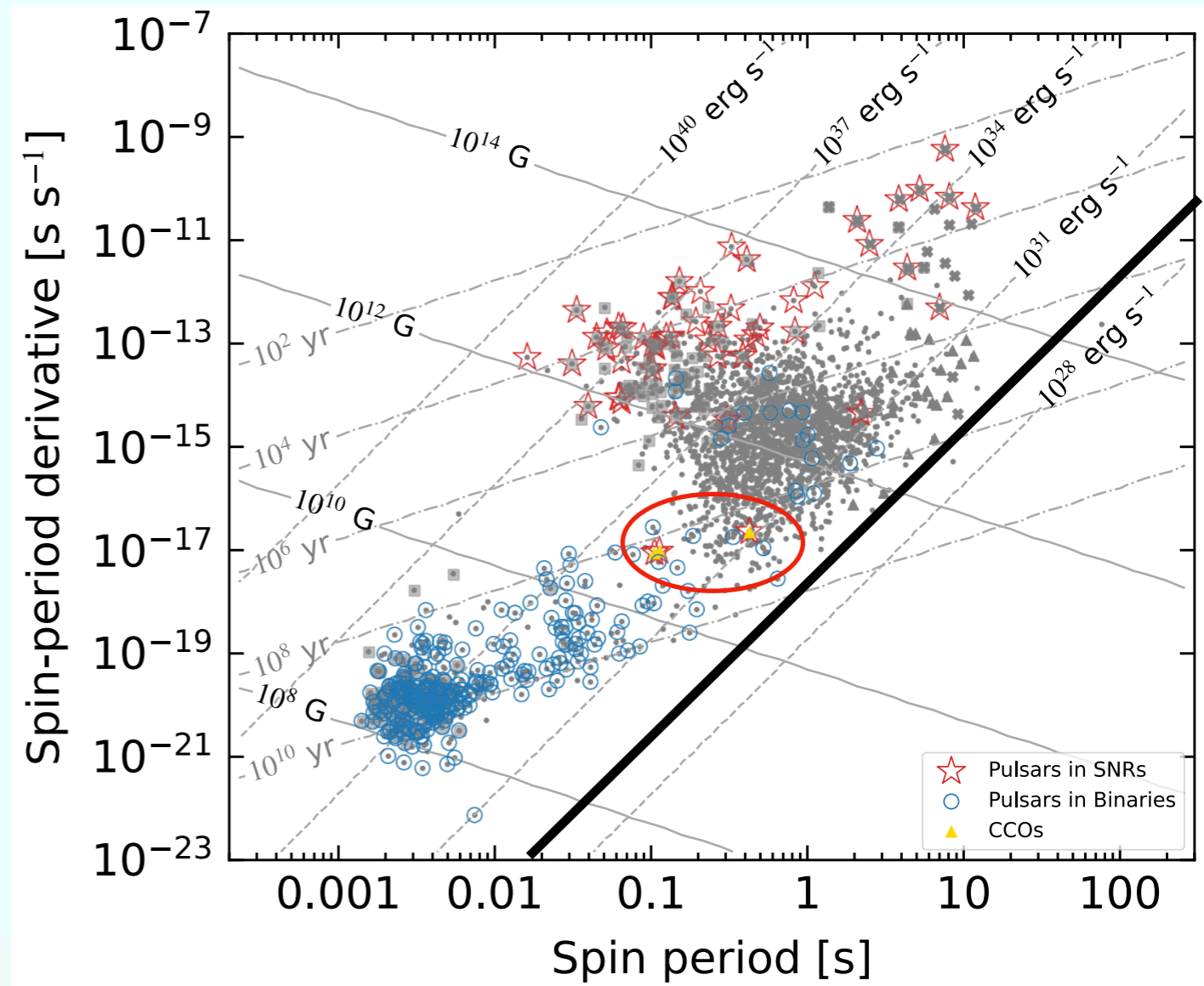
$$\tau_c \sim 10^8 \text{ yr} \gg \tau_{\text{SNR}}$$

RX J0822.0-4300, Puppis A



a.

Hui&Becker 2006



Accreting Neutron Stars

In High-mass X-ray Binaries (HMXBs)



Composed by a young neutron star accreting matter from a massive companion of spectral type O, B or Be (B stars with emission lines in the spectrum). Mass loss from the donor through stellar wind at a rate $> 10^{-5} M_{\odot} \text{ yr}^{-1}$. The wind is accreted directly to the star radially or forming a disk.

General features

$$B \sim 10^{12} - 10^{13} \text{ G}$$

$$L_X \sim 10^{34} - 10^{38} \text{ erg/s}$$

$$P \sim 0.1 - 10^4 \text{ s}$$

$$P_{\text{orb}} \sim \text{Few days-months}$$

- Usually in eccentric orbits
- Hard X-ray spectrum (0.1-100 keV)
- Regular X-ray pulsations
- Highly variable luminosity
- Optical spectrum dominated by the companion

Accreting Neutron Stars

In Low-mass X-ray Binaries (LMXBs)



Composed by a old neutron stars accreting matter from a low massive companion of spectral type K or M.or White Dwarves. Accretion via Roche Lobe overflow

General features

$$B \sim 10^8 - 10^9 \text{ G}$$

$$P \sim \text{ms} - 100 \text{ s (only a few pulsate)}$$

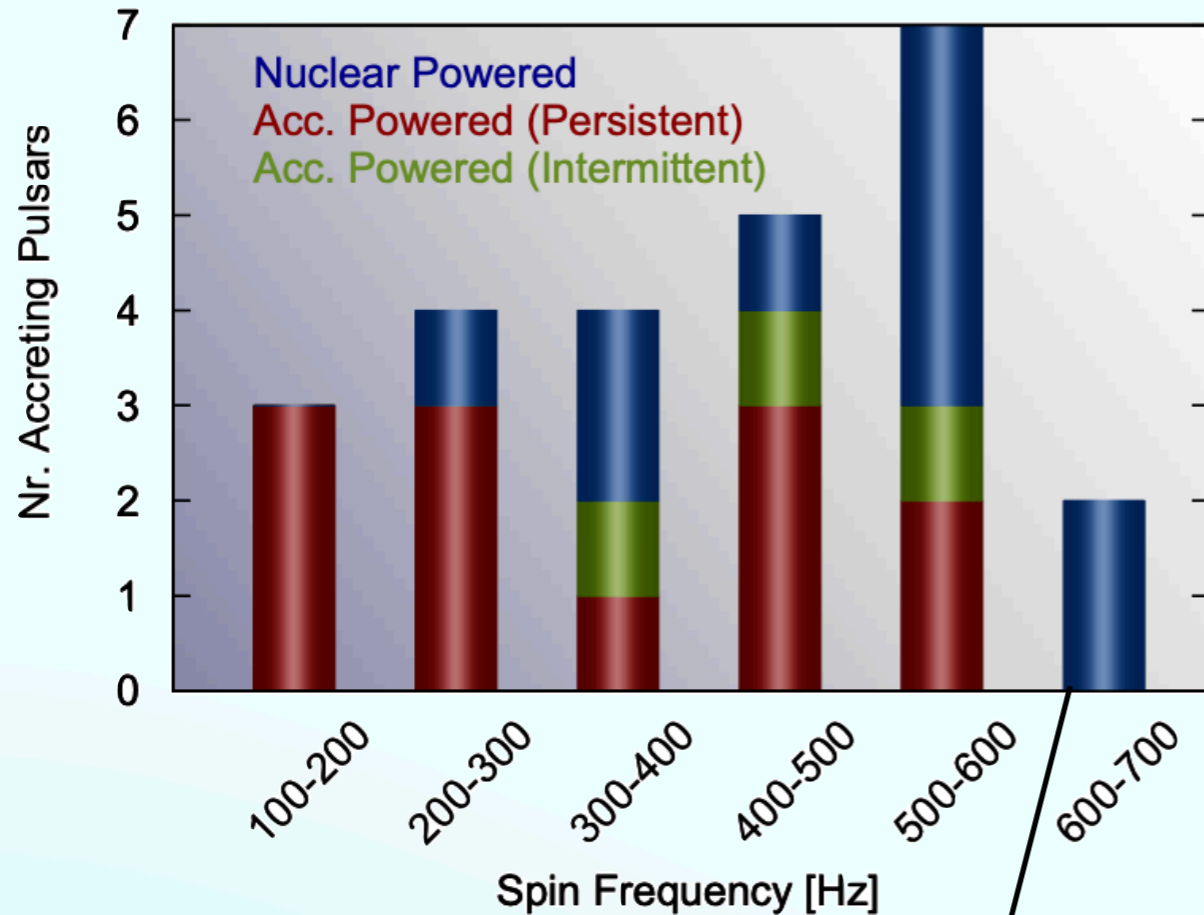
$$L_X \sim 10^{35} - 10^{38} \text{ erg/s}$$

$$P_{\text{orb}} \sim \text{minutes-days}$$

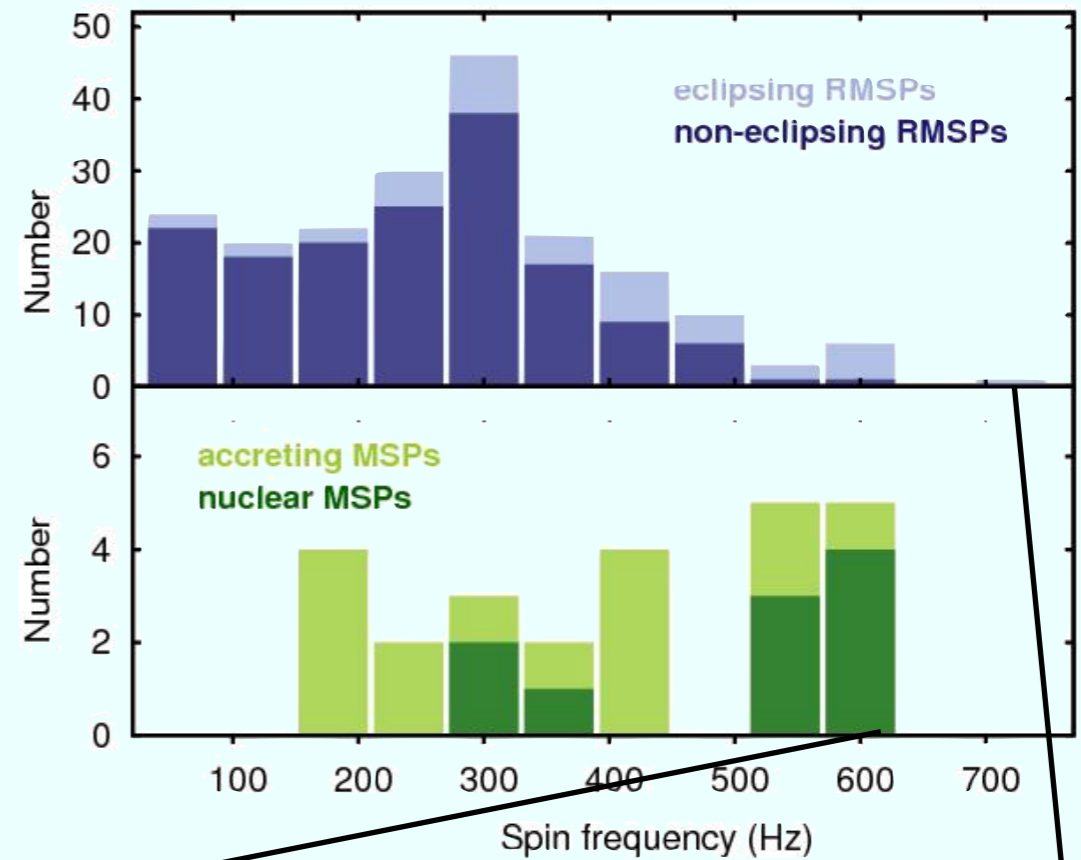
- Usually in almost circular orbits
- Soft X-ray spectrum ($kT < 15 \text{ keV}$)
- Common type I X-ray bursts
- Highly variable luminosity
- Optical spectrum dominated by reprocessed X-ray from the disk

Accreting Neutron Stars

Patruno & Watts 2021



Papitto et al. 2014



Fastest NS, 716 Hz

Abrupt cut-off at ~700 Hz. Accreting pulsars that are supposed to spin-up are spinning down or spinning up very slowly. Why?

Approximate breakup frequency for realistic equation of states (EOS)

$$\nu_{\max} \sim 1200 \text{ Hz} \left(\frac{M_{\text{NS}}}{1.4 M_{\odot}} \right)^{1/2} \left(\frac{R_{\text{NS}}}{10 \text{ km}} \right)^{-3/2}$$

Realistic EOSs support $\nu_{\max} > 1 \text{ kHz}$. Where are these rapidly rotating stars?

Additional spindown mechanism at high rotational frequency?

How Many Neutron Star?

We can estimate the total number of neutron stars in our Galaxy:

Core-Collapse
Supernova rate
 ~ 2 per century

\times

Galaxy age:
 ~ 13.6 Gyr

$=$

Neutron Star
number:
 $\sim 2.8 \times 10^8$

Birth Rate of Neutron Stars

If neutron stars originate from core collapse supernovae we expect that the rates \mathcal{R} are such that:

$$\sum_{\text{NS classes}} \mathcal{R}_i \leq \mathcal{R}_{\text{CCSN}}$$

Table 1. Estimated birthrates in units of NSs per century for the different populations of NSs. The top rows are the most likely values whereas the following rows give the lower limit pulsar current analyses for each of the pulsar current analyses.

β_{PSR}, n_e	PSRs	RRATs	XDINSs	Magnetars	Total	CCSN rate
FK06, NE2001	2.8 ± 0.5	$5.6^{+4.3}_{-3.3}$	2.1 ± 1.0	$0.3^{+1.2}_{-0.2}$	$10.8^{+7.0}_{-5.0}$	1.9 ± 1.1
L+06, NE2001	1.4 ± 0.2	$2.8^{+1.6}_{-1.6}$	2.1 ± 1.0	$0.3^{+1.2}_{-0.2}$	$6.6^{+4.0}_{-3.0}$	1.9 ± 1.1
L+06, TC93	1.1 ± 0.2	$2.2^{+1.7}_{-1.3}$	2.1 ± 1.0	$0.3^{+1.2}_{-0.2}$	$5.7^{+4.1}_{-2.7}$	1.9 ± 1.1
V+04, NE2001	1.6 ± 0.3	$3.2^{+2.5}_{-1.9}$	2.1 ± 1.0	$0.3^{+1.2}_{-0.2}$	$7.2^{+5.0}_{-3.4}$	1.9 ± 1.1
V+04, TC93	1.1 ± 0.2	$2.2^{+1.7}_{-1.3}$	2.1 ± 1.0	$0.3^{+1.2}_{-0.2}$	$5.7^{+4.1}_{-2.7}$	1.9 ± 1.1

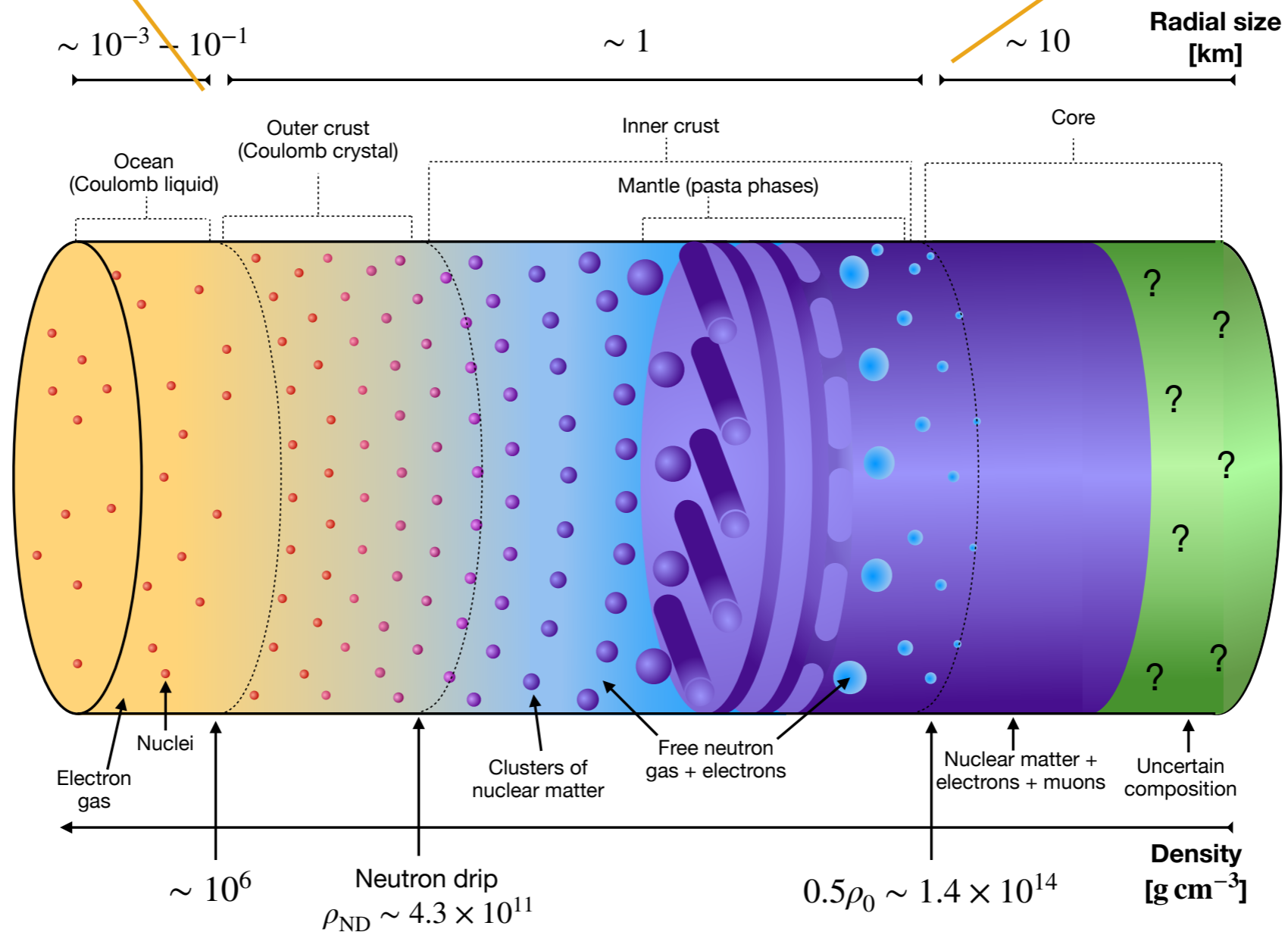
Keane & Kramer 2008

Instead we have that: $\mathcal{R}_{\text{CCSN}} < \sum_{\text{NS classes}} \mathcal{R}_i$

Magnetic field evolution

$$\frac{\partial \mathbf{B}}{\partial t} = -\nabla \times \left\{ \eta \nabla \times (e^\nu \mathbf{B}) + \frac{c}{4\pi e n_e} [\nabla \times (e^\nu \mathbf{B})] \times \mathbf{B} \right\}$$

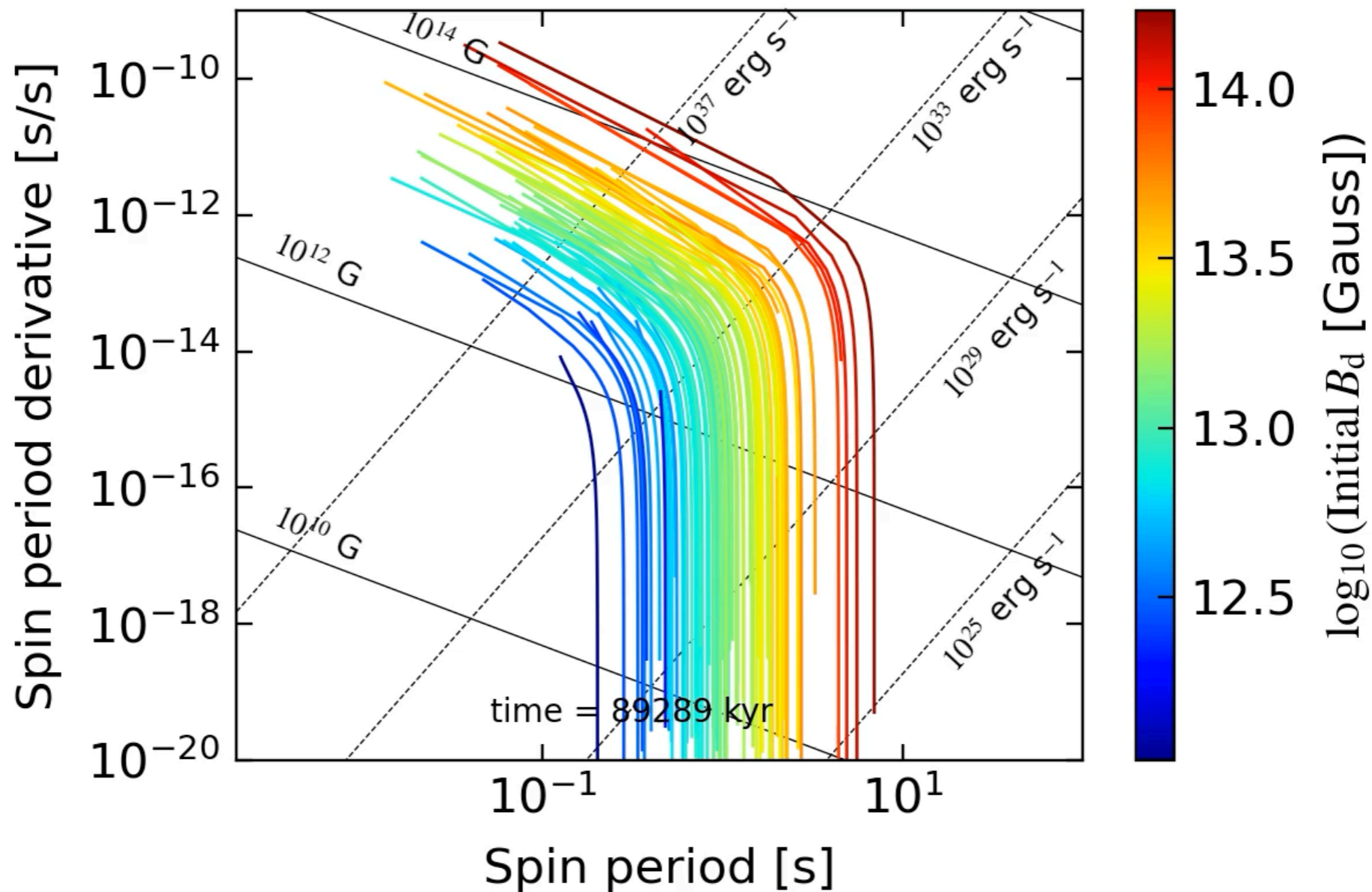
↑ Ohmic Decay
↑ Hall Drift



Magnetic field evolution

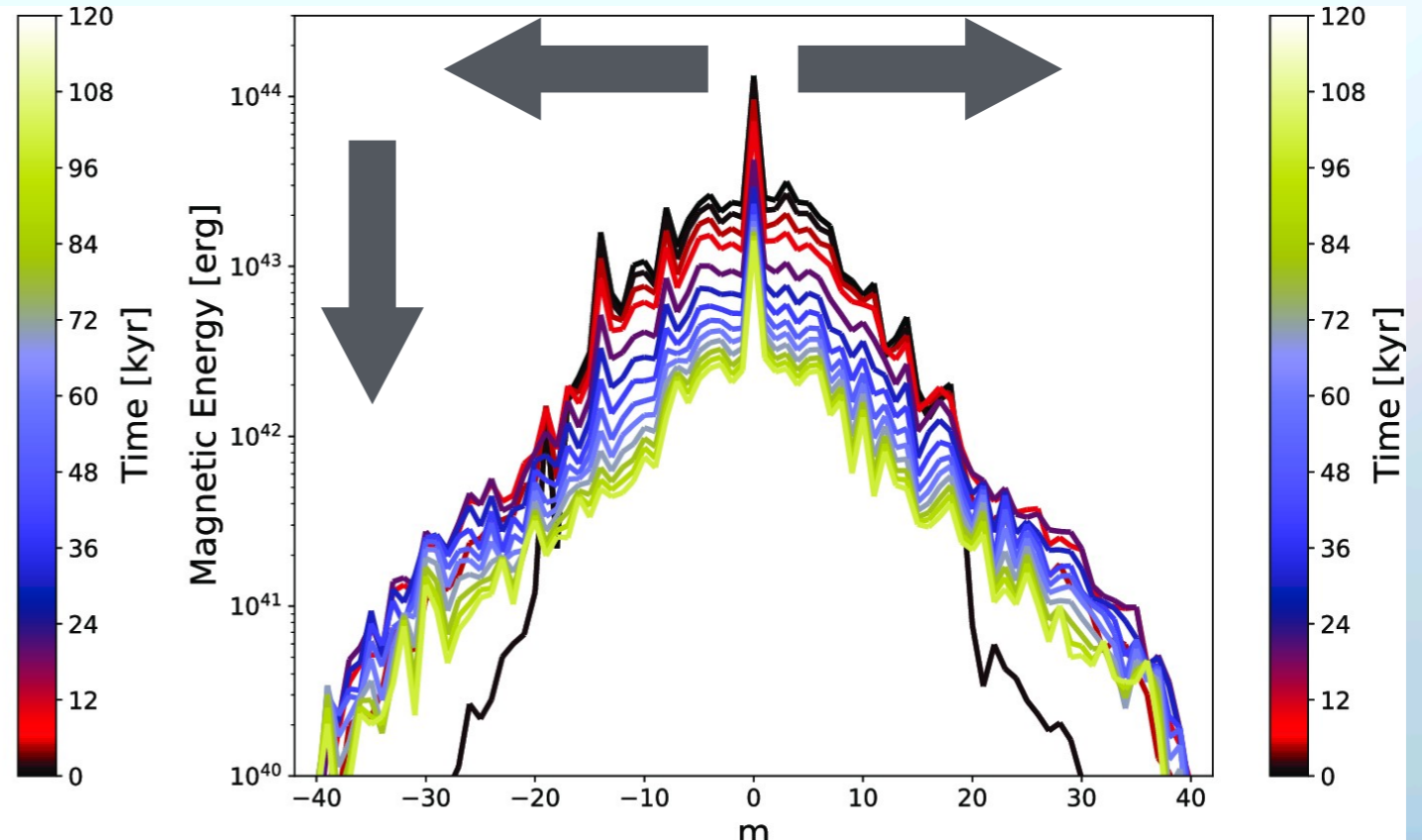
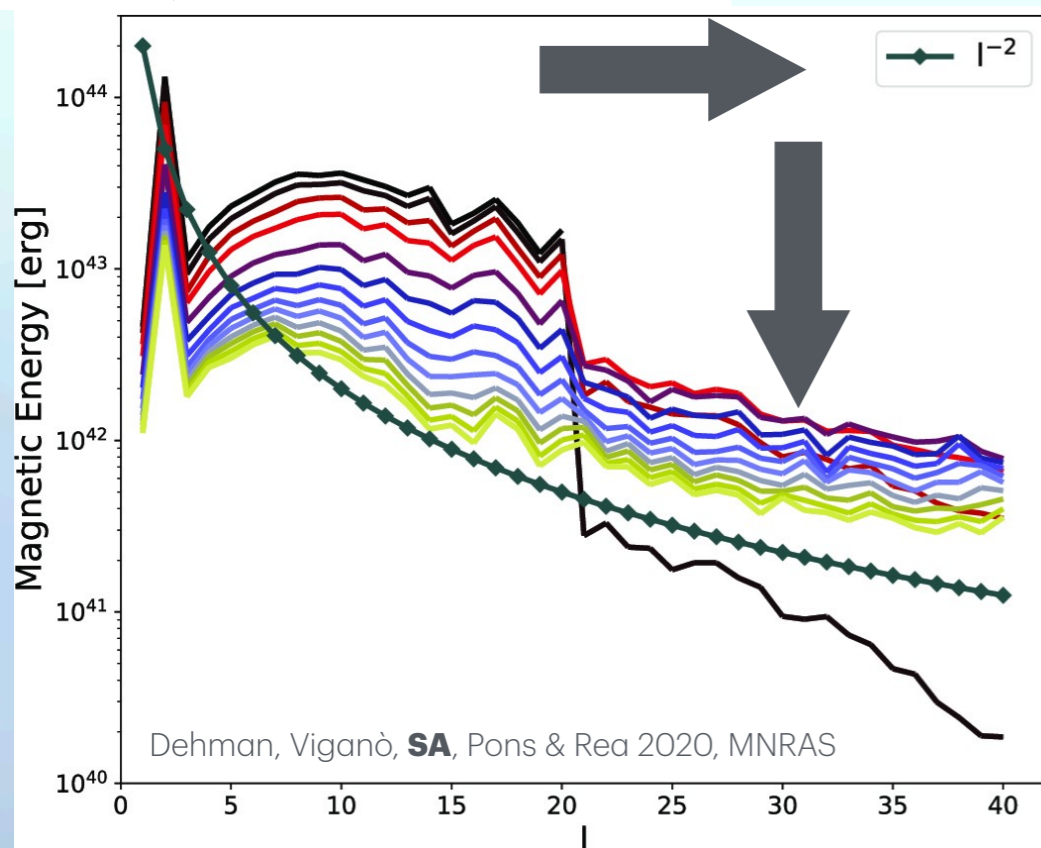
$$\frac{\partial \mathbf{B}}{\partial t} = -\nabla \times \left\{ \eta \nabla \times (e^\nu \mathbf{B}) + \frac{c}{4\pi e n_e} [\nabla \times (e^\nu \mathbf{B})] \times \mathbf{B} \right\}$$

Ohmic Decay
Hall Drift



Magnetic field evolution

$$\frac{\partial \mathbf{B}}{\partial t} = -\nabla \times \left\{ \overset{\text{Ohmic Decay}}{\eta \nabla \times (e^\nu \mathbf{B})} + \overset{\text{Hall Drift}}{\frac{c}{4\pi e n_e} [\nabla \times (e^\nu \mathbf{B})] \times \mathbf{B}} \right\}$$



Magnetic field evolution

$$\frac{\partial \mathbf{B}}{\partial t} = - \nabla \times \left\{ \eta \nabla \times (e^\nu \mathbf{B}) + \frac{c}{4\pi e n_e} [\nabla \times (e^\nu \mathbf{B})] \times \mathbf{B} \right\}$$

Magnetic Diffusivity

$$\eta = \frac{c^2}{4\pi\sigma}$$

Electric Conductivity

$$\sigma = \sigma(T)$$

The evolution of the magnetic field evolution is coupled with the evolution of the temperature

Magneto-thermal evolution required!

Magneto-thermal evolution

$$\frac{\partial \mathbf{B}}{\partial t} = - \nabla \times \left\{ \eta \nabla \times (e^\nu \mathbf{B}) + \frac{c}{4\pi e n_e} [\nabla \times (e^\nu \mathbf{B})] \times \mathbf{B} \right\}$$

$$c_\nu \frac{\partial}{\partial t} (e^\nu T) + \nabla \cdot (e^{2\nu} \mathbf{F}) = e^{2\nu} \dot{\epsilon}$$

Change of temperature in time
in an elementary volume

Heat flux through
the volume
boundary

Source therm: heat
produced/loss
within the volume

Heat can produce due to electric current (Ohmic) dissipation, rotochemical processes, vortex creep

Heat is lost due to neutrino emission

Magneto-thermal evolution

$$\frac{\partial \mathbf{B}}{\partial t} = - \nabla \times \left\{ \eta \nabla \times (e^\nu \mathbf{B}) + \frac{c}{4\pi e n_e} [\nabla \times (e^\nu \mathbf{B})] \times \mathbf{B} \right\}$$

$$c_\nu \frac{\partial}{\partial t} (e^\nu T) + \nabla \cdot (e^{2\nu} \mathbf{F}) = e^{2\nu} \dot{\epsilon}$$

We have three coupling:

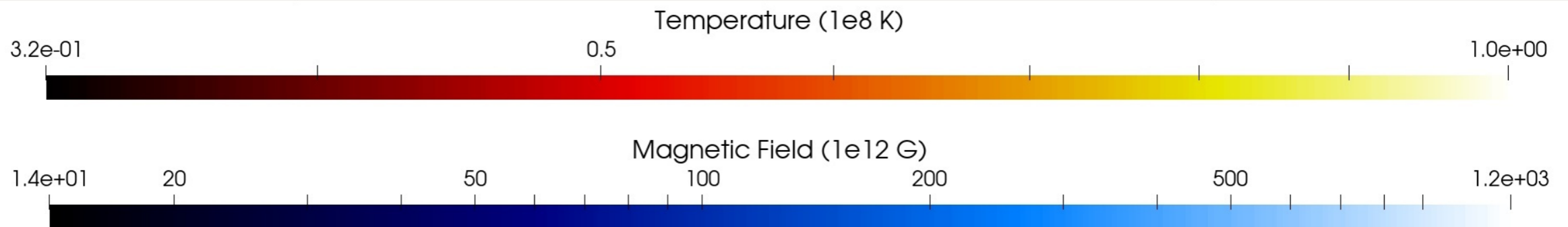
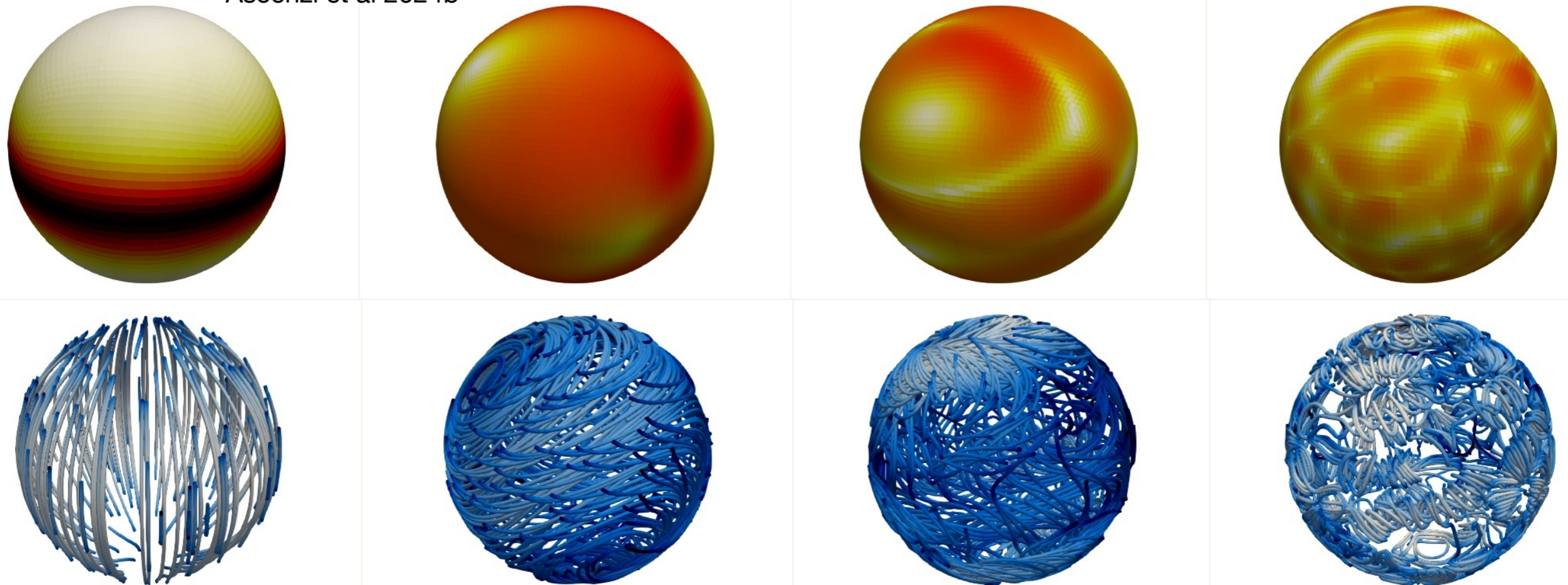
1. The magnetic diffusivity depends on the temperature
2. The source: $\dot{\epsilon} = \dot{\epsilon}_h - \dot{\epsilon}_\nu$. The magnetic field dissipation is a source of heat and some neutrino synchrotron-like processes depends on the magnetic field
3. The thermal conductivity becomes anisotropic in presence of a strong magnetic field

Magneto-thermal evolution



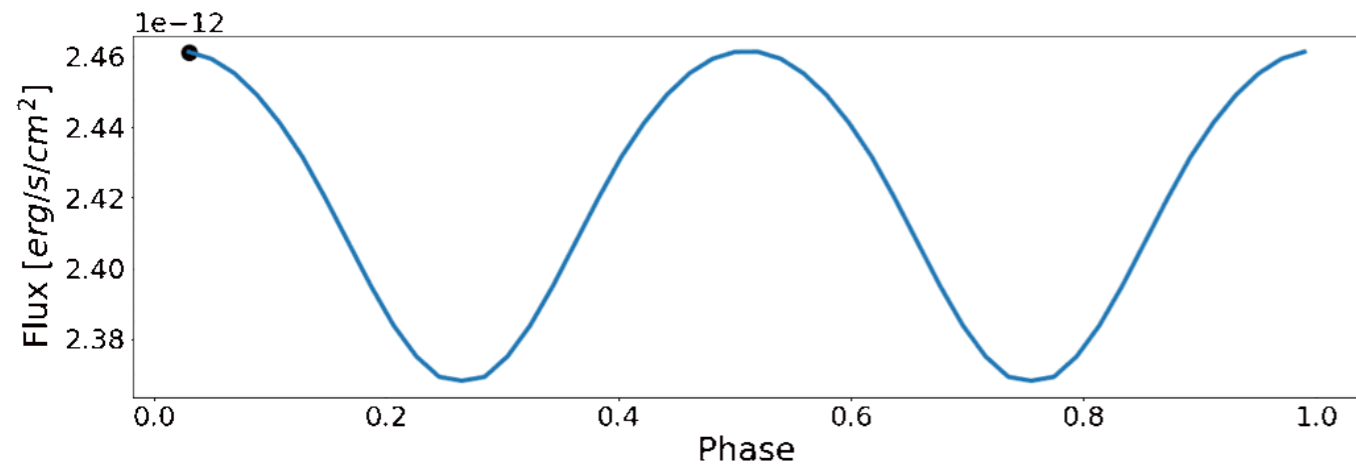
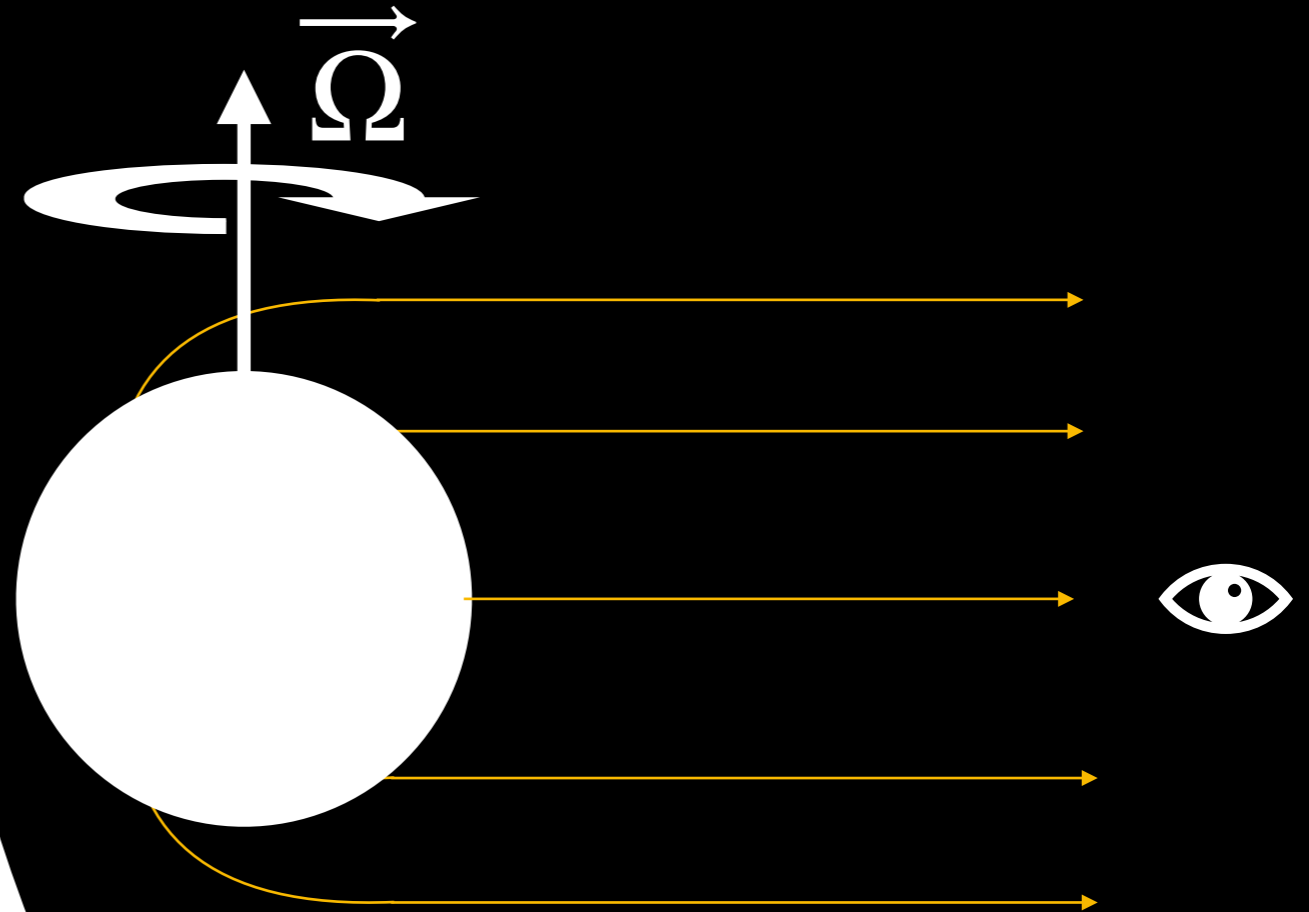
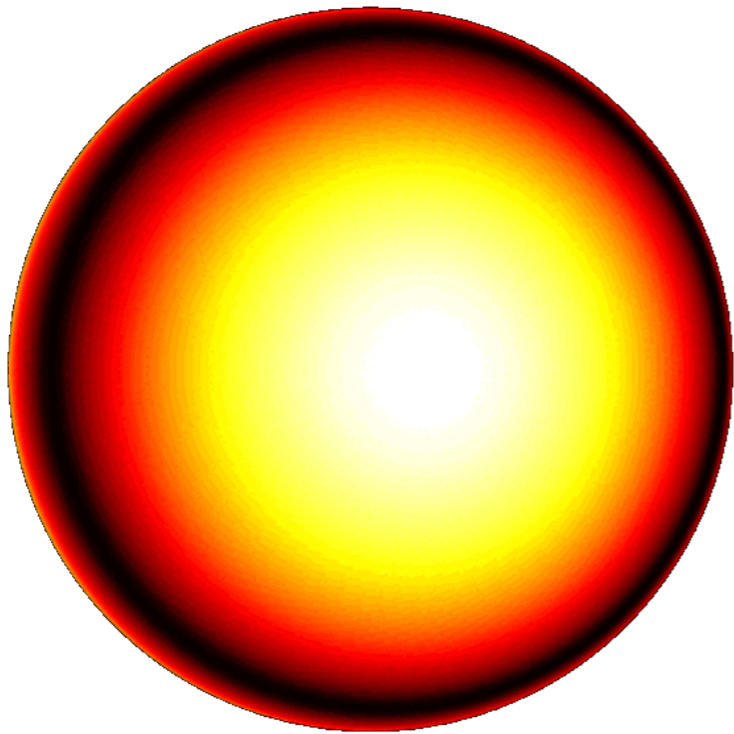
Ascenzi et al 2024b

The magnetic field leads to the formation of inhomogeneities after a few years in the temperature of an initially homogeneous NS crust.



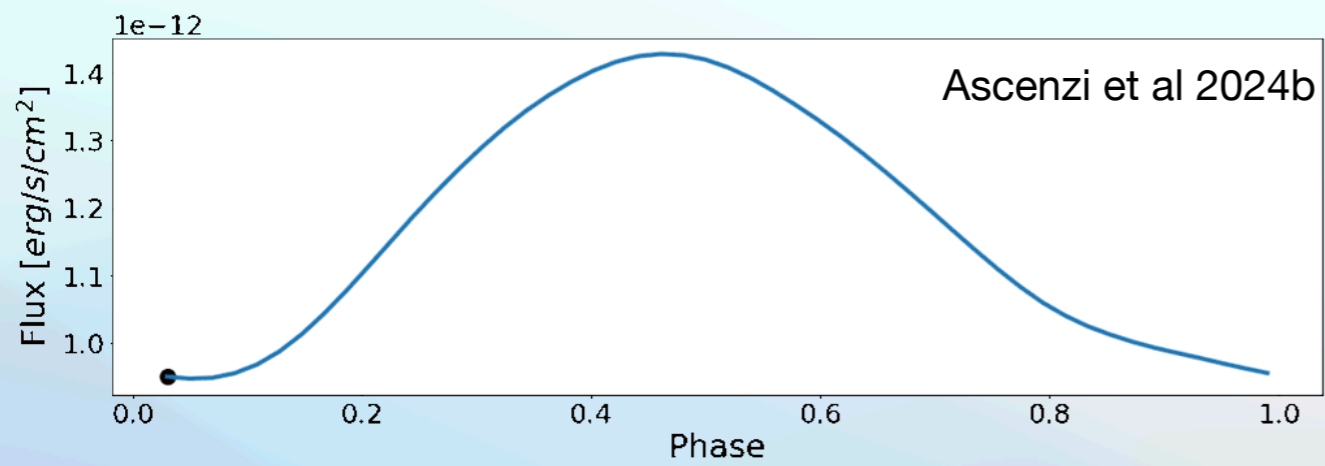
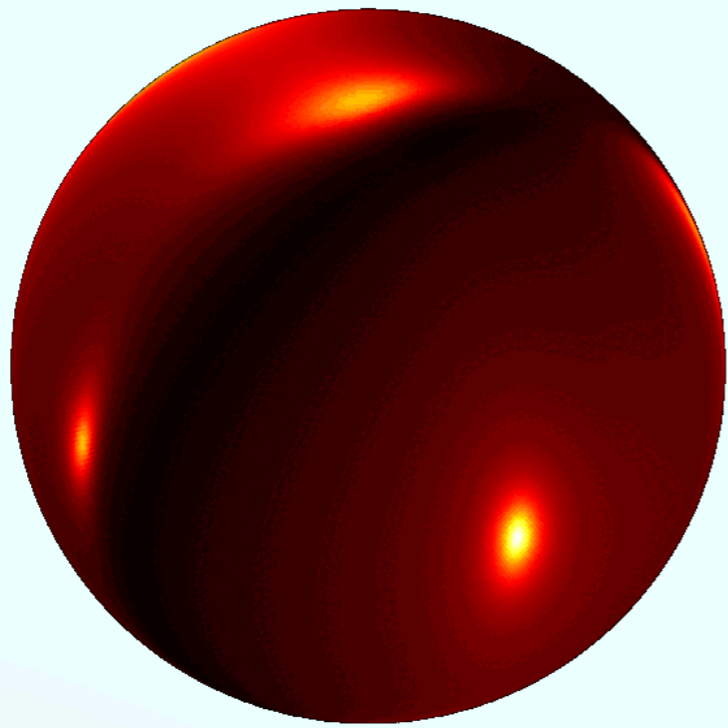
In collaboration with Prof. Rosalba Perna (Stoney Brook University)

We use a **ray-tracing code** to model pulsating thermal emission from magnetars

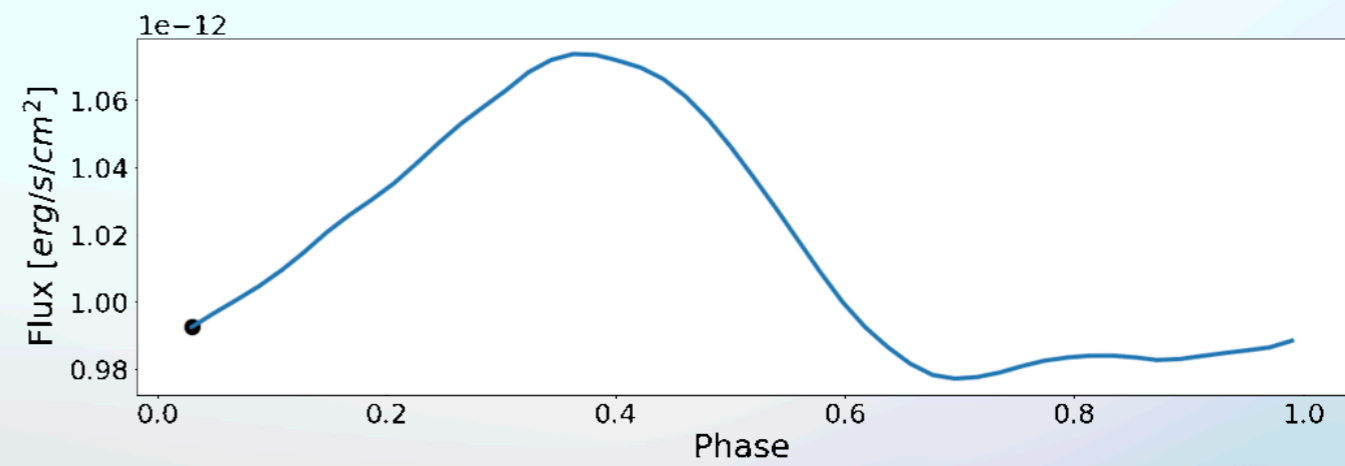
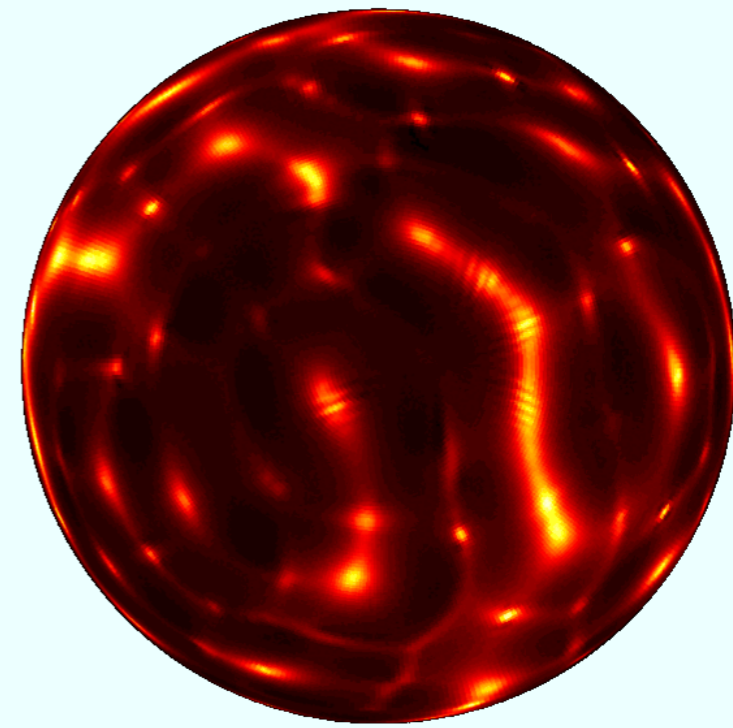


Ascenzi et al 2024b

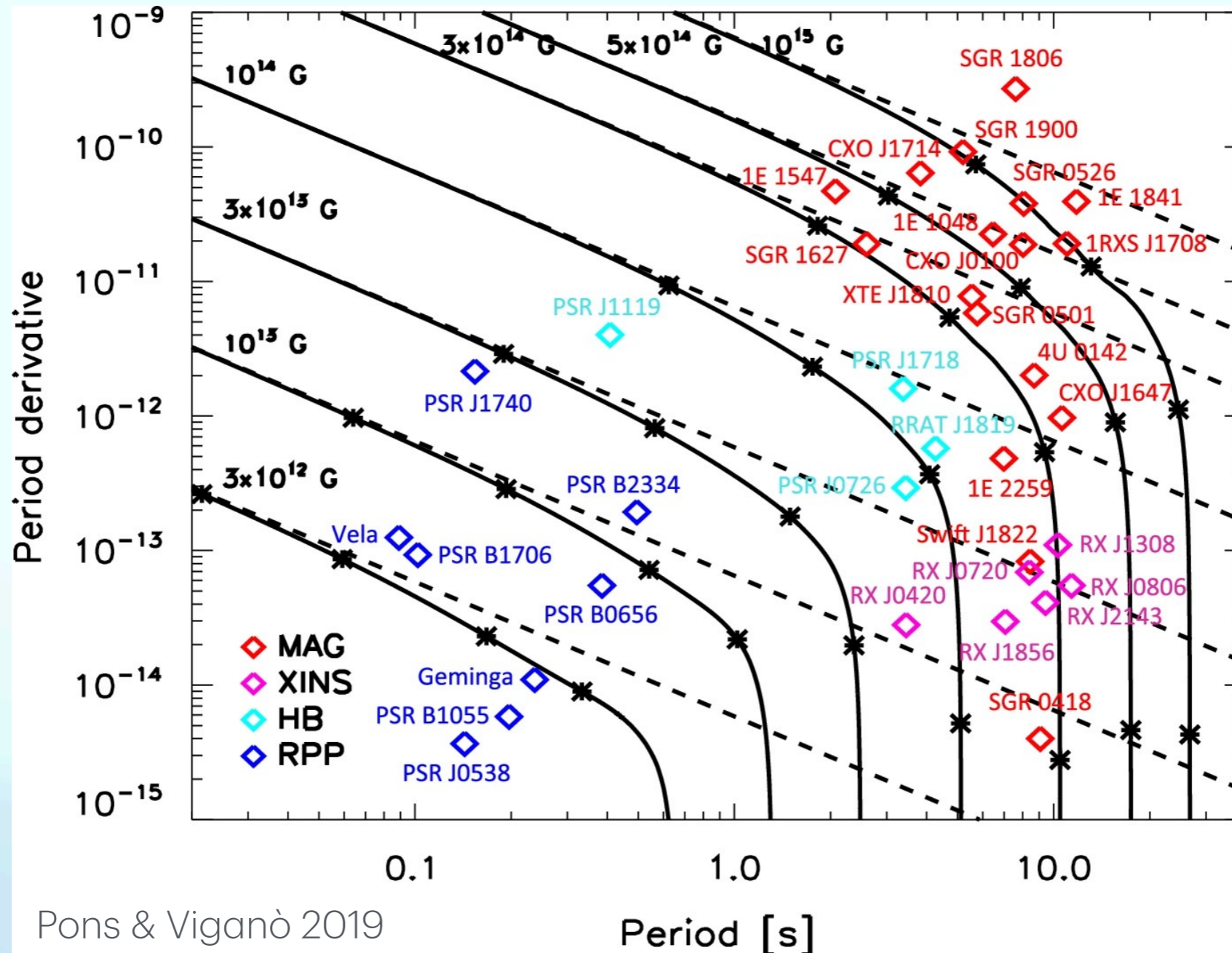
Pulsed Fraction $\sim 20\%$



Pulsed Fraction $\sim 4\%$



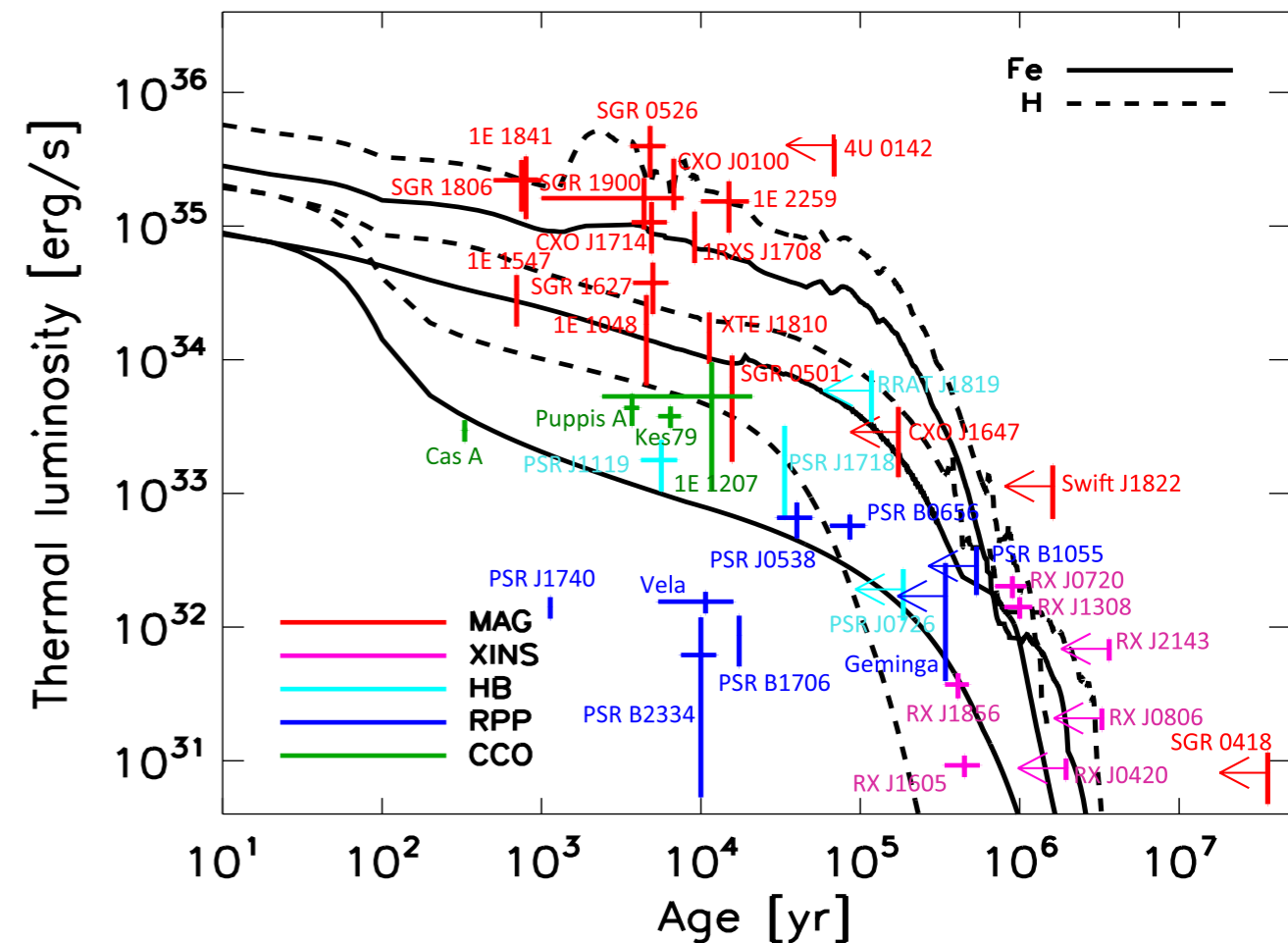
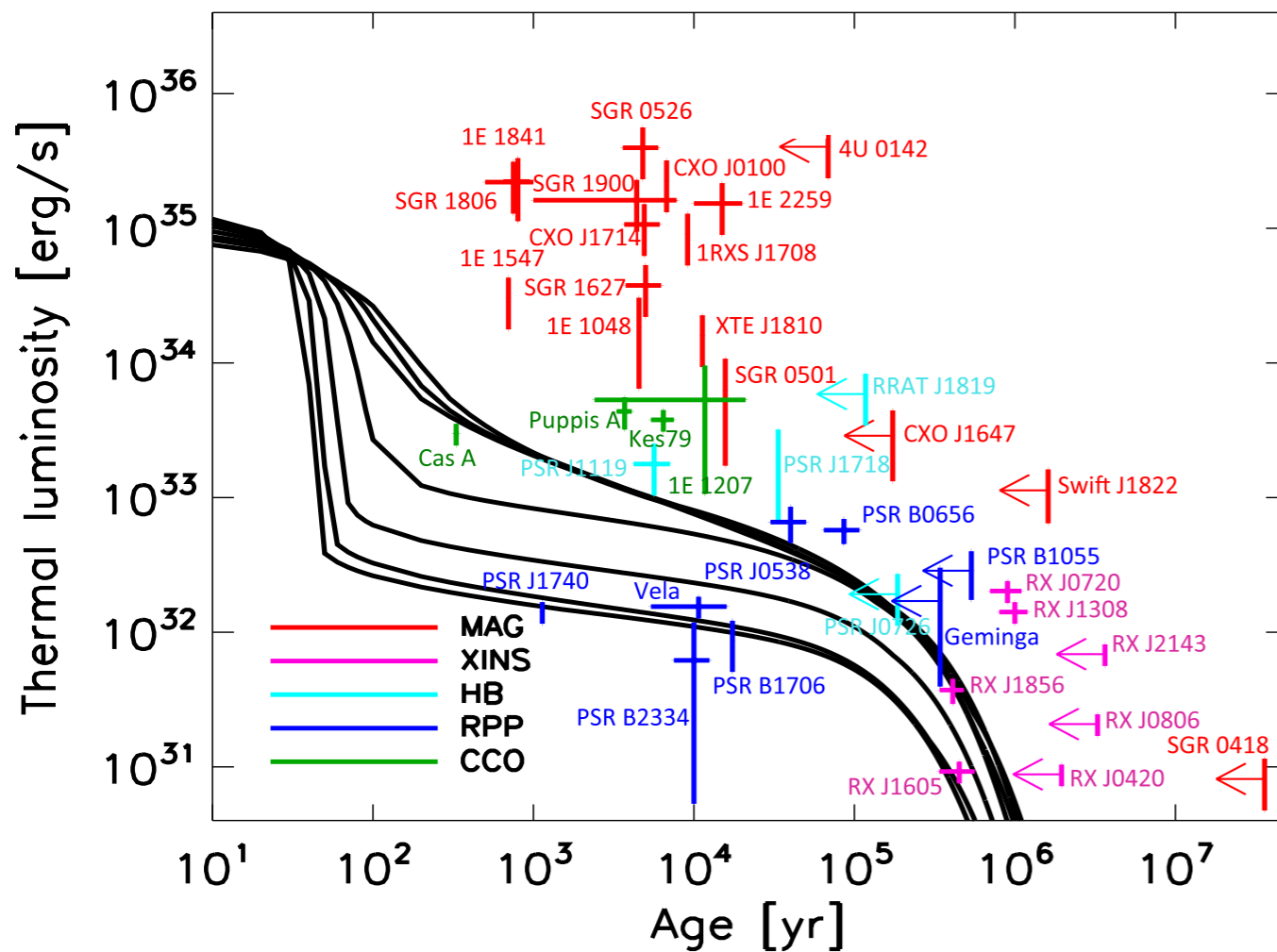
Magneto-thermal evolution



XDINS are on evolutionary tracks of magnetars in $P - \dot{P}$ diagram!

Magneto-thermal evolution

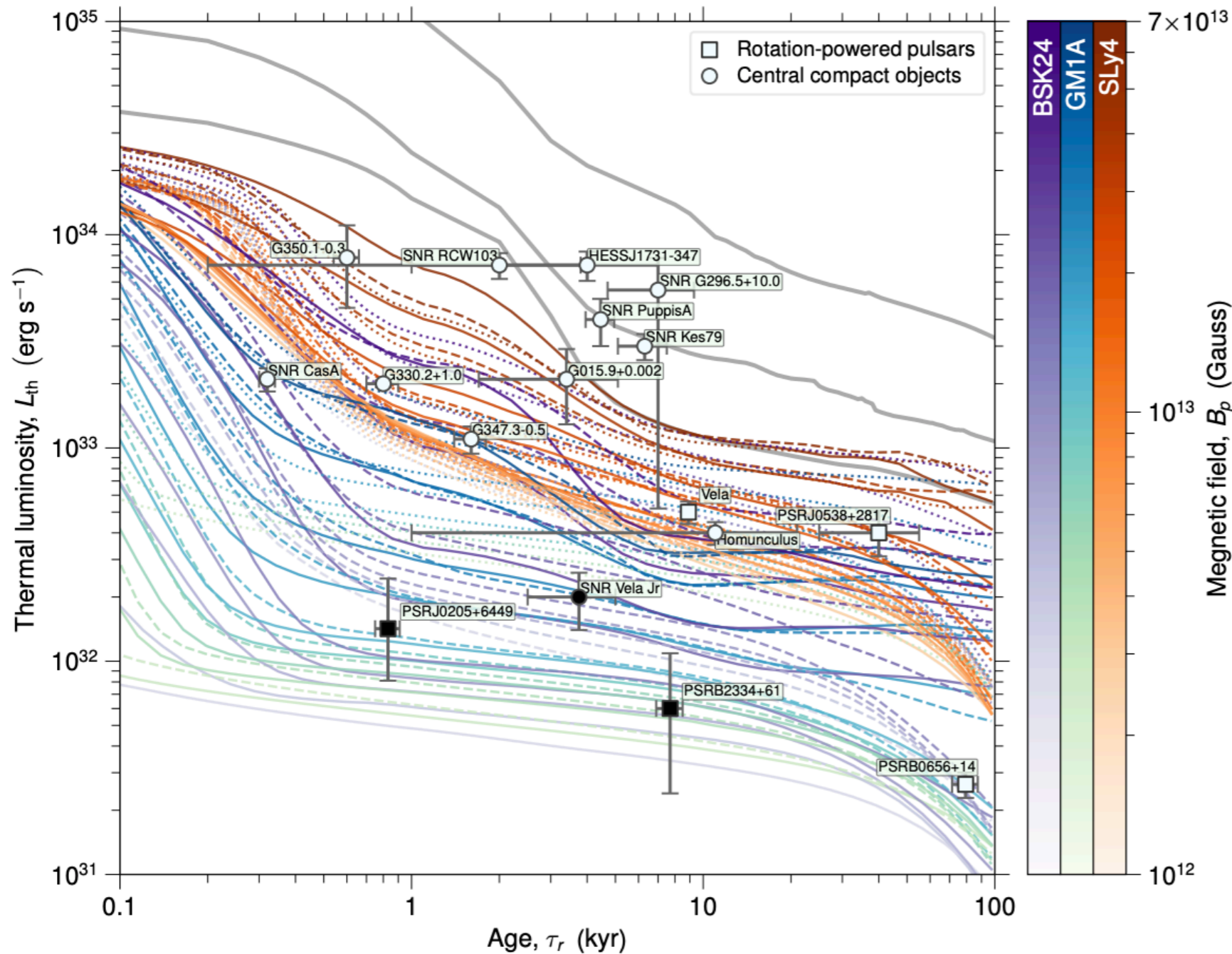
Magnetic field dissipation
required to account for hot
NS



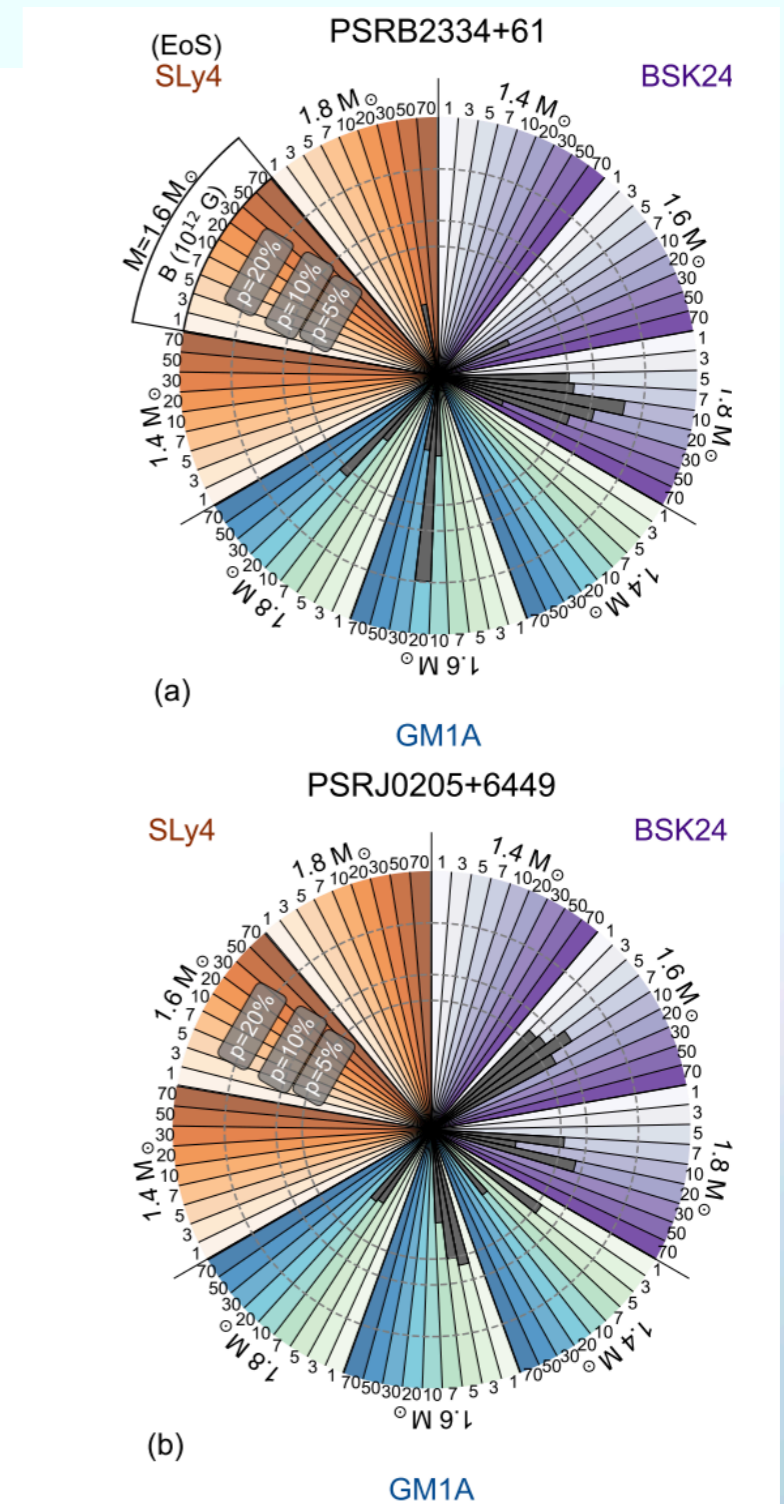
Efficient Cooling mechanisms
required to account for cold
young stars

Magneto-thermal evolution

The cooling can constrain the EOS!



Marino et al. 2024



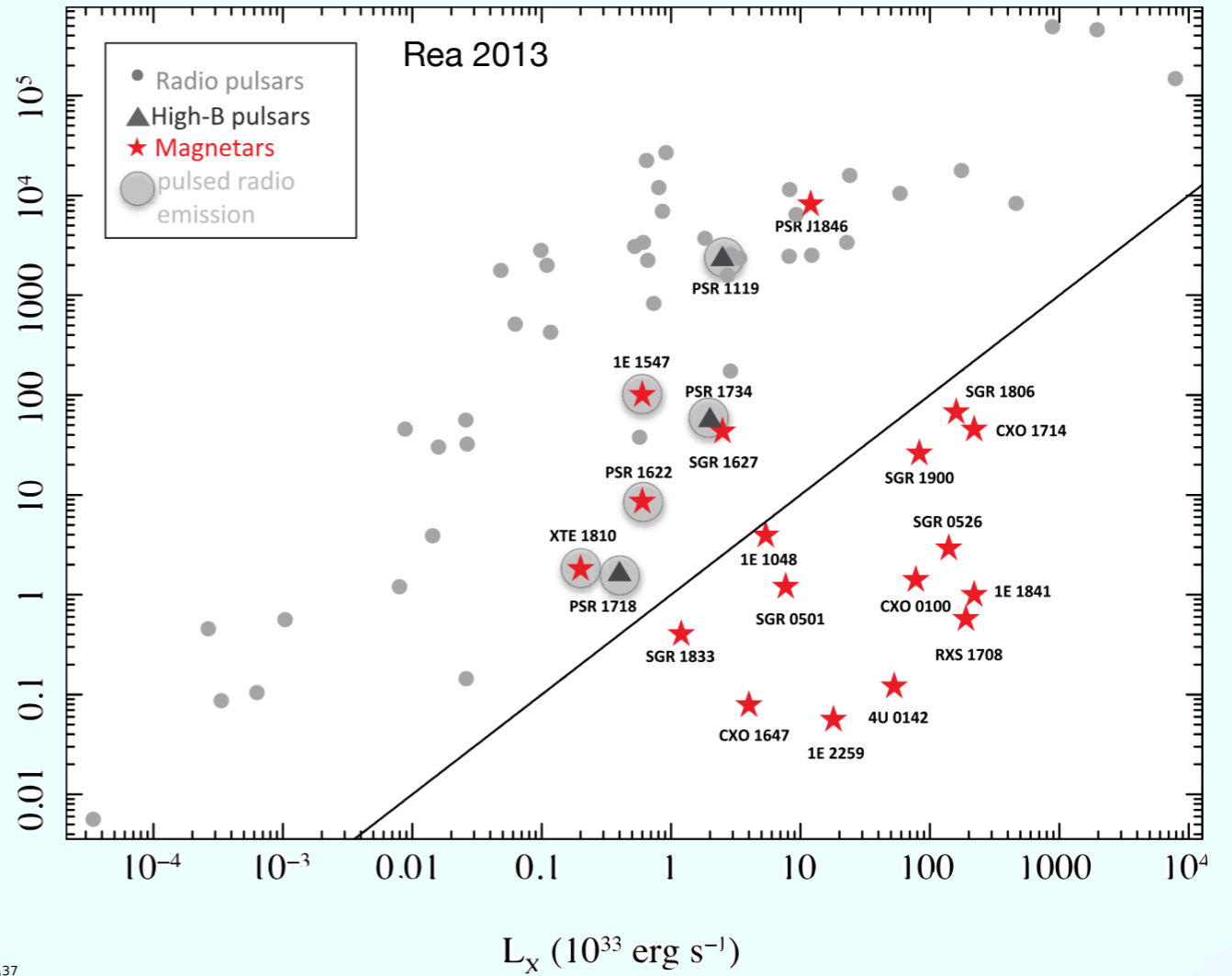
Summary

- Neutron stars appear divided in different classes presenting different observational features
- The total birthrate of different neutron star populations seems in tension with the rate of core-collapse supernovae
- One possible solution is that different classes of neutron stars are related to each other within a unified evolutionary path
- Magneto-thermal simulations allows to probe this framework and to constrain neutron star EOSs

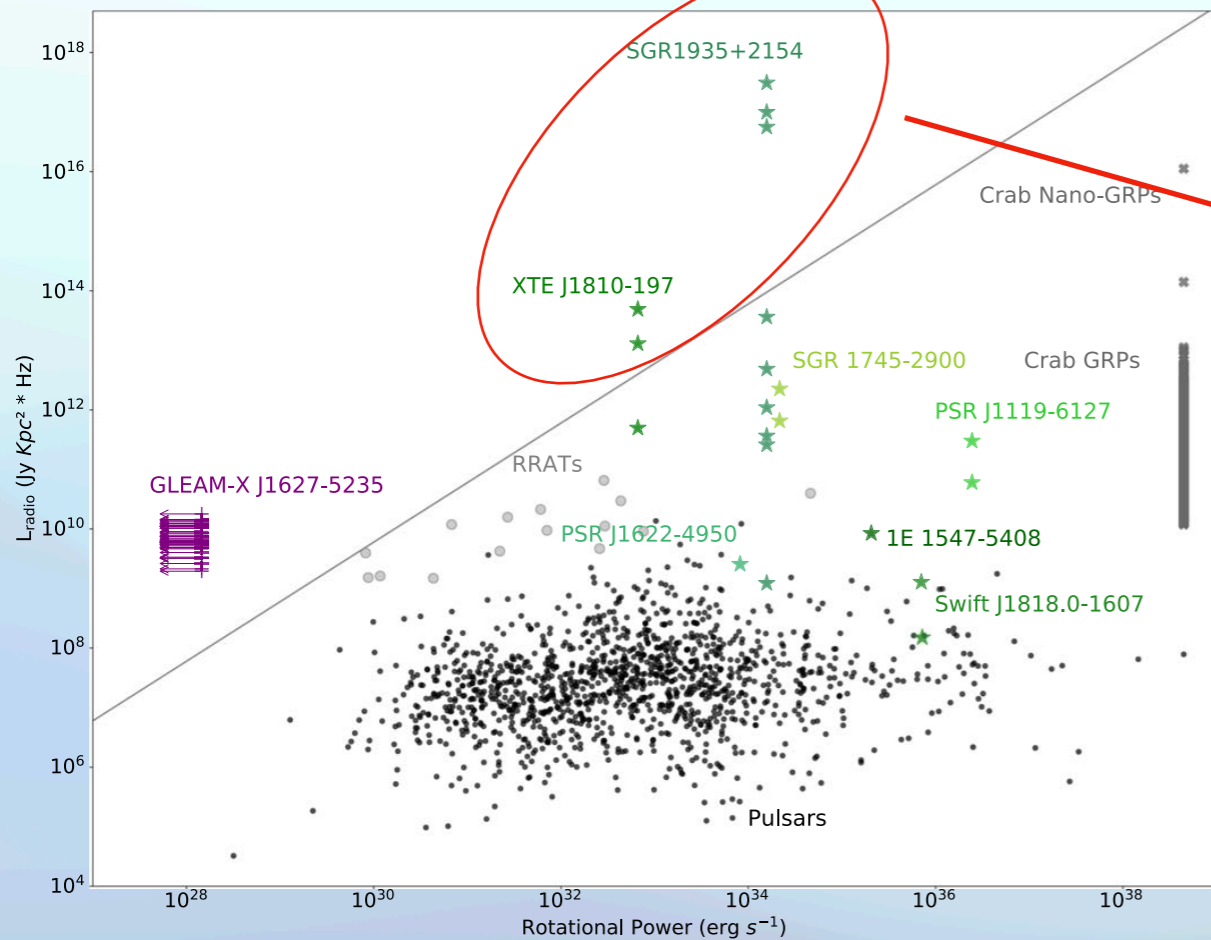
Thank you for your attention!



Magnetars

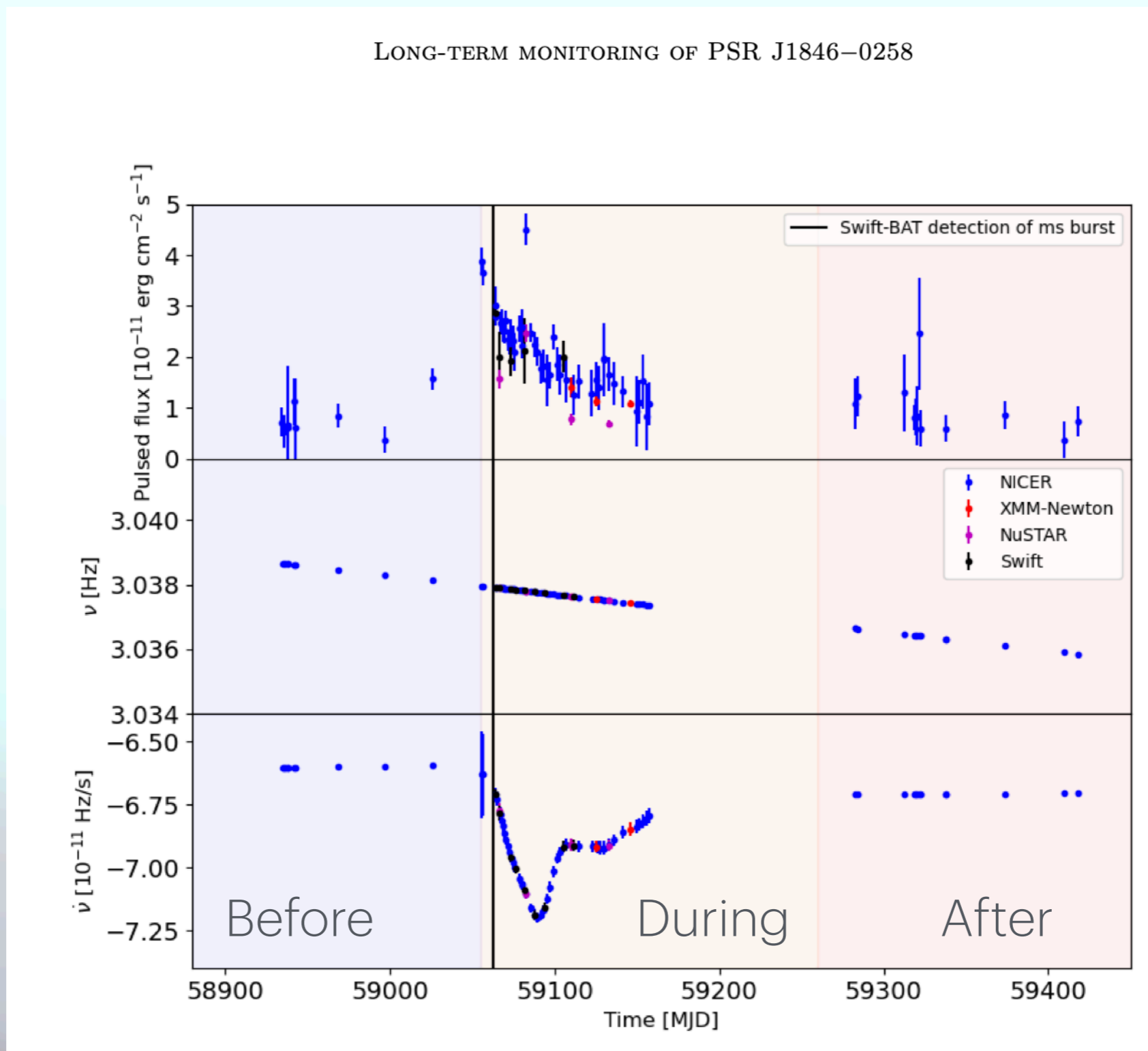


Rea et al. 2022



Magnetar Radio Bursts with luminosity higher than spindown power

Magnetars in outburst



X-ray Dim Isolated Neutron Stars (XDINSs)

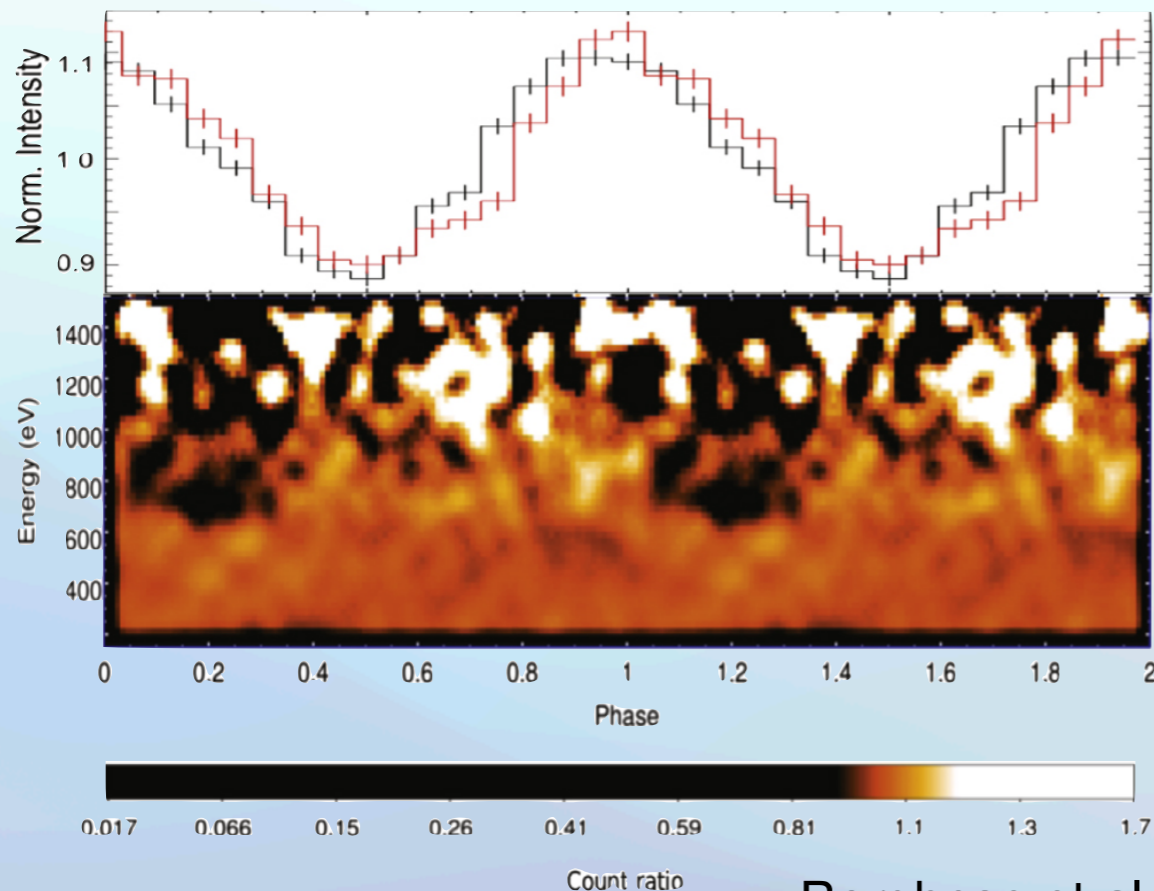
RX J0720.4-3125

Blackbody spectrum

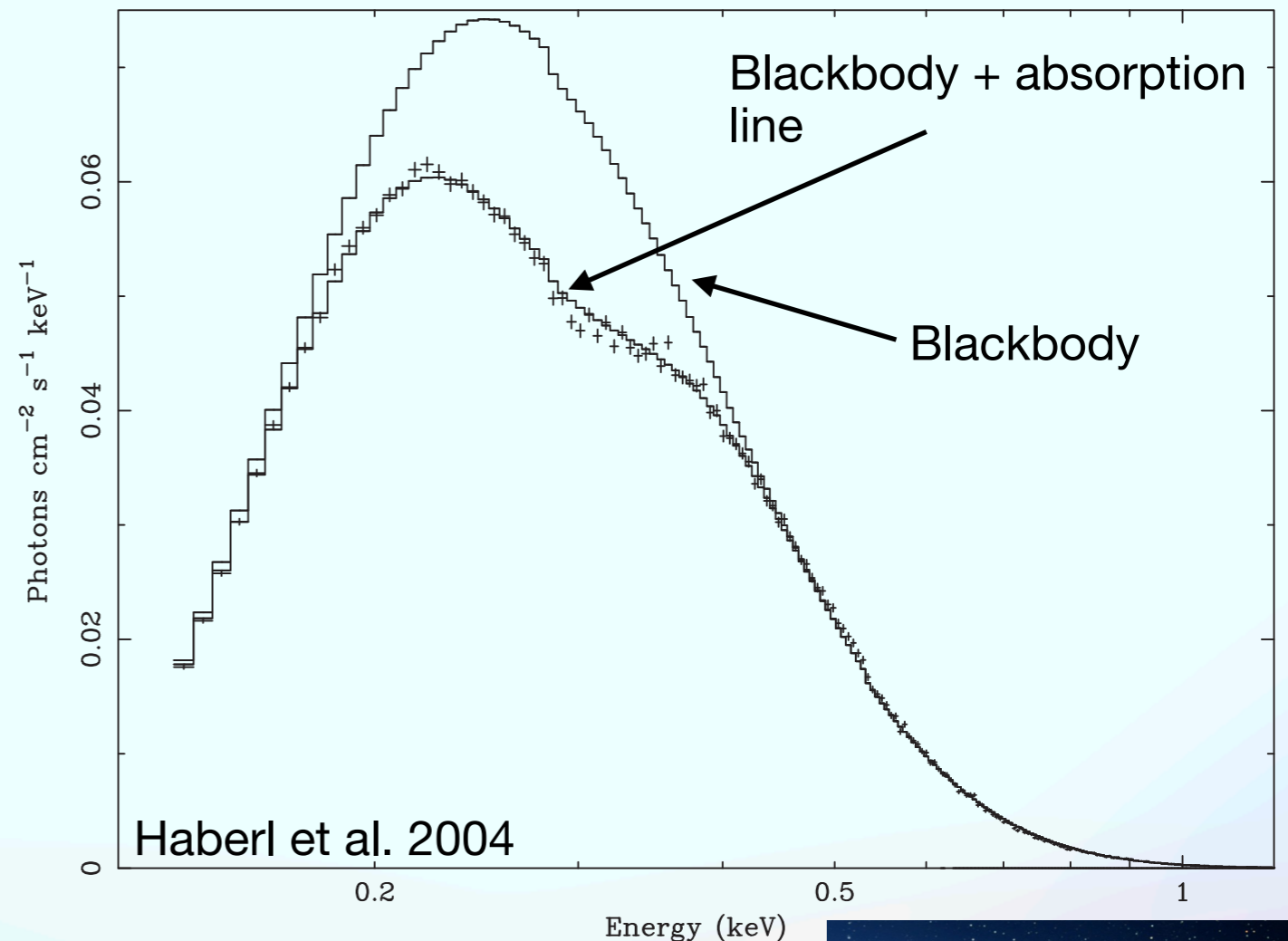
$$kT_{BB} \sim 50 - 100 \text{ eV}$$

plus a broad absorption feature

$$E_{\text{line}} \sim 0.2 - 0.8 \text{ keV}$$



Borghese et al. 2015

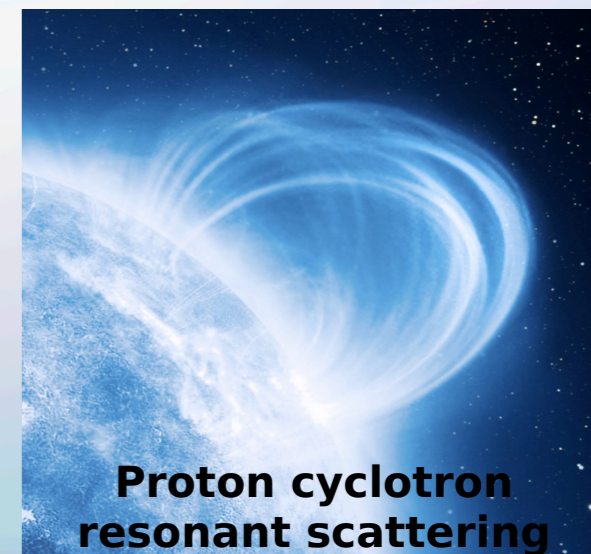


Haberl et al. 2004

← Phase dependent narrow absorption feature

$$B_{\text{dip}} \sim 2.5 \times 10^{13} \text{ G}$$

$$B_{\text{loop}} \sim 1.8 \times 10^{14} \text{ G}$$



Proton cyclotron resonant scattering

How Many Neutron Star?

We can estimate the total number of neutron stars in our Galaxy:

$$\begin{array}{ccc} \begin{array}{c} \text{Core-Collapse} \\ \text{Supernova rate} \\ \sim 2 \text{ per century} \end{array} & \times & \begin{array}{c} \text{Galaxy age:} \\ \sim 13.6 \text{ Gyr} \end{array} & = & \begin{array}{c} \text{Neutron Star} \\ \text{number:} \\ \sim 2.8 \times 10^8 \end{array} \end{array}$$

We can only detect a very small fraction of all neutron stars. **Population synthesis** bridges this gap focusing on the full population of neutron stars (eg. Faucher-Giguère & Kaspi 2006, Lorimer et al. 2006, Gullón et al. 2014, Cieřlar et al. 2020)

model birth
properties with
Monte-Carlo
approach

Evolve
properties
forward in time

Apply filters to
mimic
observational
biases/limits

Compare mock
simulations to
observations to
constrain input

Dynamical Evolution

- Neutron stars are born in star-forming regions, i.e., in the Galactic disk along the Milky Way's spiral arms, and receive kicks during the supernova explosions.
- We make the following assumptions:
 - Electron-density model (Yao et al., 2017) + rigid rotation with $T = 250$ Myr.
 - Exponential disk with scale height $h_c = 0.18$ kpc (Wainscoat et al., 1992).
 - Single-component Maxwell kick-velocity distribution with dispersion $\sigma_k = 265$ km/s (Hobbs et al., 2005).
 - Galactic potential (Marchetti et al., 2019).



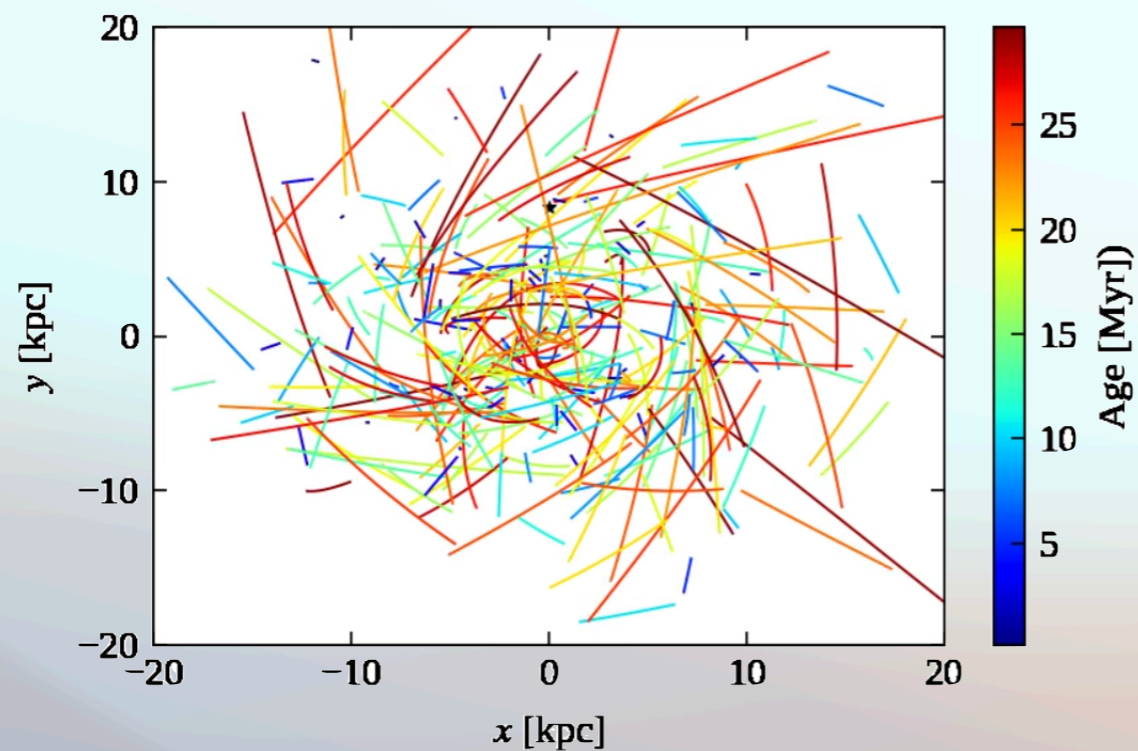
We use this information to determine pulsar positions and velocities

Dynamical Evolution

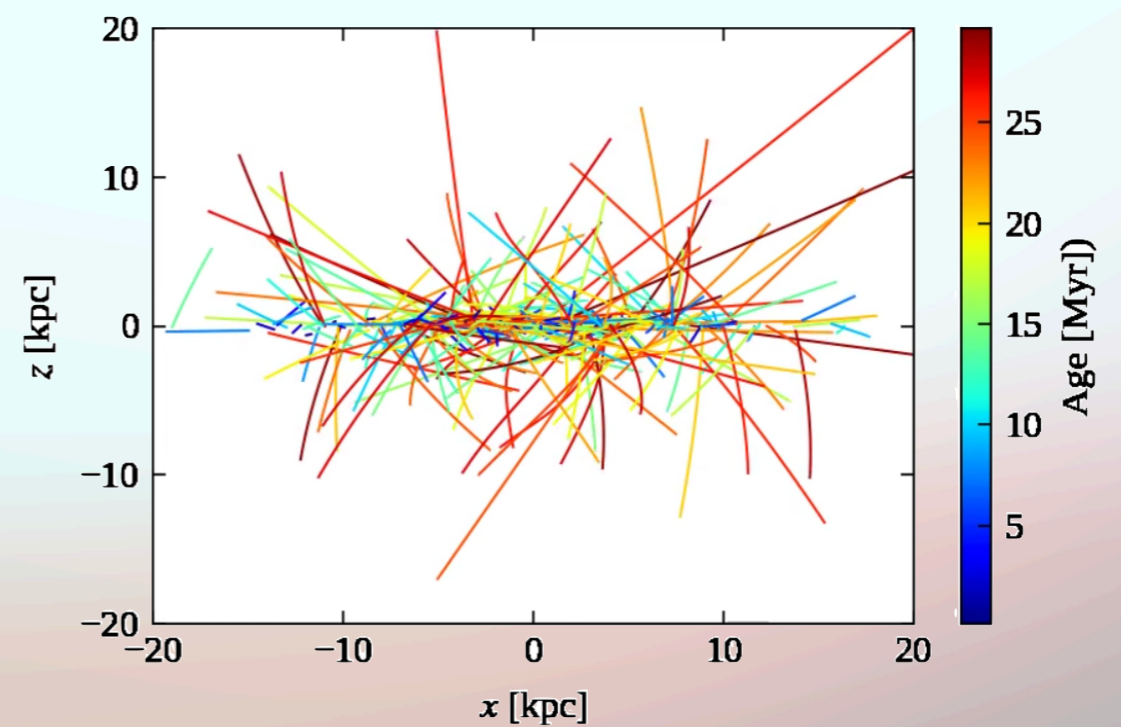
- For our Galactic model Φ_{MW} , we evolve the stars' position & velocity by solving Newtonian equations of motion in cylindrical galactocentric coordinates:

$$\ddot{\vec{r}} = -\vec{\nabla}\Phi_{\text{MW}}$$

Top View



Side View



Galactic evolution tracks for $h_c = 0.18 \sigma = 265 \text{ km/s}$

Magneto-Rotational evolution

The NS magnetosphere exerts a torque onto the star. This causes spin-down and the alignment of the magnetic and rotational axis

$$\dot{P} = \frac{\pi^2 B^2 R^6}{c^3 IP} (k_0 + k_1 \sin^2 \chi)$$

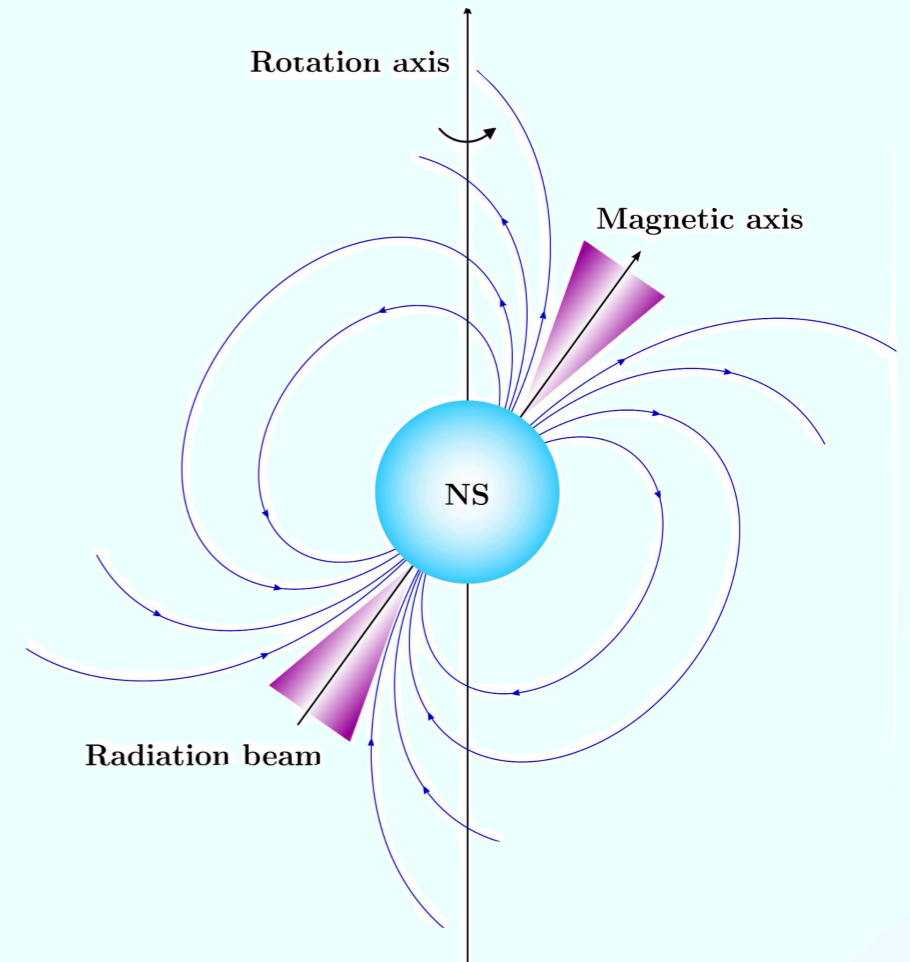
(Spitkovsky 2006)

$$\dot{\chi} = -\frac{\pi^2 B^2 R^6}{c^3 IP^2} (k_2 \sin \chi \cos \chi)$$

(Philippov, Tchekhovskoy & Li 2014)

We make the following assumptions:

- Initial periods follow a log-normal with $\mu_{\log P}$ and $\sigma_{\log P}$ (Igoshev et al. 2022)
- Initial fields follow a log-normal with $\mu_{\log B}$ and $\sigma_{\log B}$ (Gullón et al. 2014)



But the magnetic field decay due to Ohmic dissipation and Hall effect in the crust! (e.g. Viganò et al. 2013)

Above $\tau \sim 10^6$ yr fields decay follows a power-law with $B(t) \sim B_0(1 + t/\tau)^a$

Five parameters: $\mu_{\log P}$, $\sigma_{\log P}$, $\mu_{\log B}$, $\sigma_{\log B}$ and a

Magneto-Rotational evolution

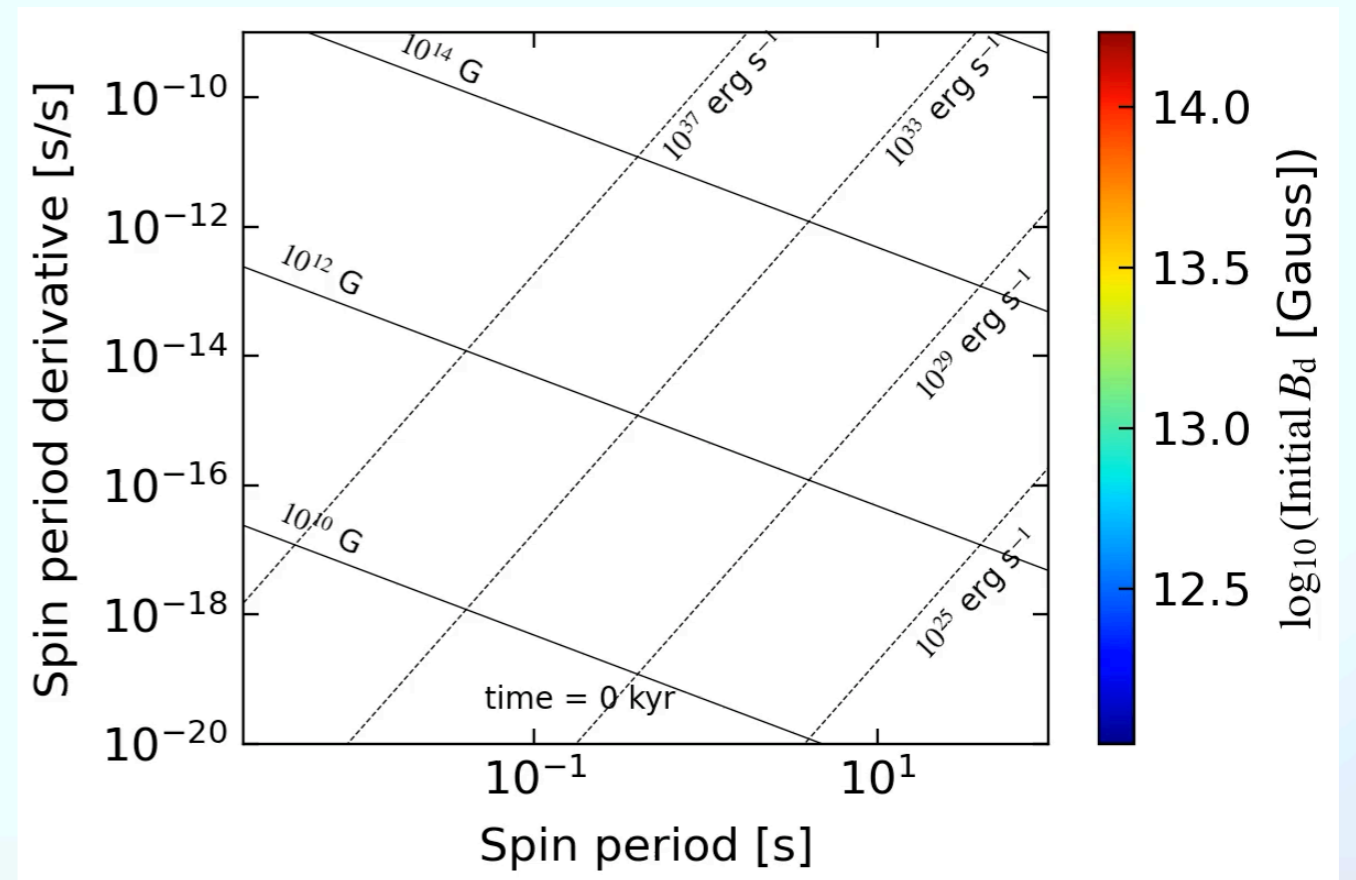
To model the magneto-rotational evolution, we numerically solve two coupled ordinary differential equations for the period and the misalignment angle

$$\dot{P} = \frac{\pi^2 B^2 R^6}{c^3 IP} (k_0 + k_1 \sin^2 \chi) \quad (\text{Spitkovsky 2006})$$

$$\dot{\chi} = -\frac{\pi^2 B^2 R^6}{c^3 IP^2} (k_2 \sin \chi \cos \chi) \quad (\text{Philippov, Tchekhovskoy \& Li 2014})$$

We use results from magneto-thermal simulations to determine the evolution of the magnetic field.

This allows us to follow the stars' P and \dot{P} in the $P - \dot{P}$ diagram



Some Results...

